Journal of the Palaeontological Society of India
Volume 67(1), June 30, 2022: 93-112

ISSN 0552-9360

Incisor enamel microstructure of some Neogene muroid rodents of India: taxonomic, evolutionary and biomechanical implications

Ankita Singla[1], Rajeev Patnaik[1*], Ningthoujam Premjit Singh[2], K. Milankumar Sharma[3] & Ashok Sahni[1]

JPSI

The fossil muroid rodent record of the Indian subcontinent is deep-rooted and is based mainly on isolated molars. However, rodent incisors from the Neogene terrestrial sequences of the subcontinent have rarely been studied for their taxonomic, evolutionary, and adaptive applications. Based on a detailed analysis of their enamel microstructure, we assign the rodent incisors from the middle Miocene Siwaliks of Ramnagar (J&K), to murine (cf. *Antemus*), cricetine and rhizomyine (cf. *Kanisamys*) and those from the late Miocene deposits of Kachchh (Gujarat) to murine (cf. *Progonomys*), rhizomyine (cf. *Kanisamys*), ctenodactyline (cf. *Sayimys*) and sciurine (cf. *Tamias*). Early and late Pliocene Siwalik rodent incisors have been assigned to murine (cf. *Nesokia,* cf. *Millardia,* cf. *Mus,* cf. *Bandicota,* cf. *Golunda*), gerbilline (cf. *Abudhabia*) and rhizomyine (cf. *Rhizomys*). Our study reveals that the Siwalik cricetid incisors differ from those of other murine incisors in possessing surface ornamentation. Murines are characterized by having smooth enamel surface with transversely to partly transverse and partly diagonally arranged HSBs with angled to perpendicular IPM. Compared to this, gerbillines show wide grooves/sulci on the enamel surface while rhizomyines have three to four-layered enamel structures. In *Antemus*-*Progonomys*-*Mus* lineage, *Antemus* shows round prism cross-section, transverse HSBs and angled IPM, while *Progonomys* and *Mus* show oval prism cross-section, transverse and diagonal HSBs, and almost perpendicular IPM. Biomechanically, cf. *Antemus* and a few other murines with thin modified radial enamel may suggest a diet of hard substances. Rhizomyines like cf. *Kanisamys* and cf. *Rhizomys*, and murines such as cf. *Nesokia* and cf. *Bandicota* shows thicker outer enamel indicating digging and burrowing behaviours.

ARTICLE HISTORY

Manuscript received: 19/02/2022
Manuscript accepted: 12/04/2022

Keywords: Neogene, Muroids, Enamel Microstructure, Taxonomy, Biomechanics.

[1]Department of Geology, Panjab University, Chandigarh 160014, India; [2]Wadia Institute of Himalayan Geology, Dehradun-248001, India; [3]Department of Geology, Central University of Punjab, Bathinda-151001, India. Corresponding author e-mail: rajeevpatnaik@gmail.com*

INTRODUCTION

Rodents are characterized by their ever-growing incisors and exhibit all the stages of tooth formation at any given point in time (Fig. 1). Rodents depend heavily on their ever-growing incisors for gnawing, cutting, burrowing, digging and food gathering. The mechanical strength of the incisor enamel depends on its microstructure, which has evolved in response to the adaptive radiation of rodents (Flynn, 1977). The taxonomy and phylogeny of rodents are based mainly on the molar morphology which has evolved rather rapidly providing characteristic features for the identification of taxa up to genus and species levels. In the fossil record, molars are usually less abundant as compared to the ever-growing, mostly fragmented incisors. At the family level, incisors are considered more useful for comparative phylogenetic and taxonomic studies, because all rodent species have roughly the same shape of incisors and are not strongly influenced by different biomechanical constraints. Moreover, in contrast to molars, incomplete and fragmented incisors are good enough for enamel microstructural studies.

Enamel is confined to the anterior side (labial) of an incisor and may in some taxa extend slightly on the mesial and distal sides (Fig. 1). The upper and lower jaws have two incisors each and are mirror images of each other. The upper and lower incisors wear against each other producing sharp chisel-shaped edges. Their tips have mature old enamel and distal parts have young and immature enamel. Some rodents acquired ornamental features independently on their upper incisors like deep grooves/ridges/ribs running along the length of the enamel, which can be useful for taxonomic differentiation (Flynn, 1977).

Enamel is highly resistant, mineralized and is the hardest tissue that can be produced by vertebrates. Dental enamel is made up of tightly packed prisms of hydroxyapatite crystallites (all with the same orientation), which are deposited by ameloblast in all mammals. During amelogenesis, prisms originate from the enamel-dentine junction (EDJ) (Fig. 4B) and migrate towards the outer surface of the enamel and bend sharply towards the tip of incisors (Schroeder, 1987). These prisms are surrounded by parallelly-oriented hydroxyapatite crystals known as 'Interprismatic Matrix' (IPM) (also see Fig. 2B). The IPM may run parallel (in primitive rodents), at an acute angle or perpendicular (in the most advanced

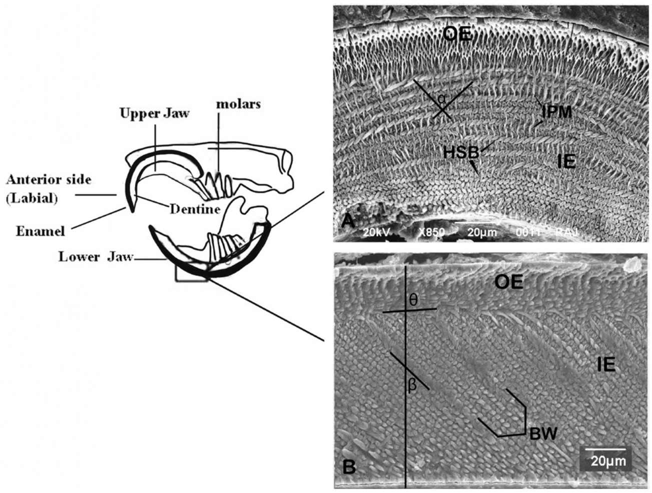

Fig. 1. SEM micrographs of extant rodent species, *Mus musculus* (VPL/PU/MMT1) showing various enamel features, OE- Outer enamel, IE- Inner enamel, BW- Band width, α- Decussation angle, β-Incisal inclination, θ-Outer enamel prism inclination, HSB- Hunter-Schreger Bands, IPM- Inter-Prismatic Matrix. A. Transverse section (Scale-20 µm), B. Longitudinal section (Scale-20 µm).

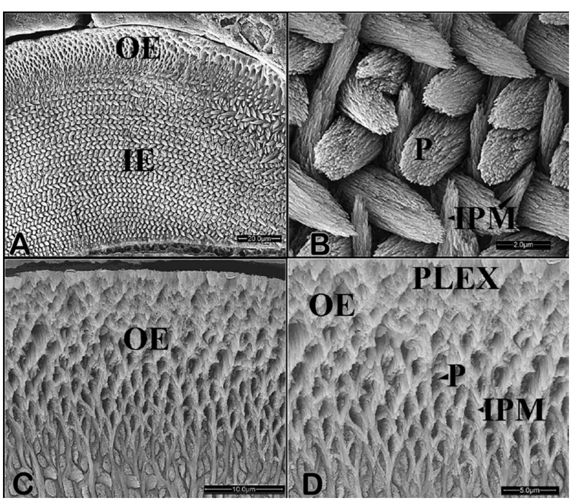

Fig. 2. SEM micrographs of transverse sections of lower incisor of extant rodent species *Mus musculus* (VPL/PU/MMT1) showing A, inner enamel (IE), outer enamel (OE); B, the magnified portion of inner enamel showing prisms (P), Inter-Prismatic Matrix (IPM); C, outer enamel magnified and D, magnified outer enamel showing Prism less External Layer (PLEX), prisms and inter-prismatic matrix.

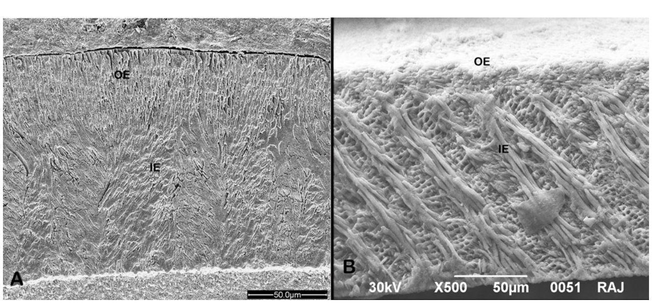

Fig. 3. SEM micrographs of rodent incisors showing A. Pauciserial enamel in lower incisor of cf. *Birbalomys* VPL/AS/Ka-1 from the Subathu Formation (Eocene) of Kalakot (J&K) (Scale-50µm), B. Multiserial enamel in lower incisor of cf. *Sayimys* VPL/AS/KU-16 from Kachchh (Gujarat).

rodents) to the prisms, a feature found useful in assessing phylogenetic relationships (Martin, 1992, 1993). A distinct prism boundary called 'prism sheath' is formed due to the different orientations of prism and interprismatic crystallites. Enamel is divided into two layers, Portio Interna (inner) and Portio Externa (outer) (Fig. 1A & B). In the Outer Enamel, prisms run parallel to each other forming 'Radial Enamel' (Fig. 2C & D), which is considered to be the most original form of enamel pattern (Koenigswald and Clemens, 1992; Kalthoff, 2000). In the Inner Enamel, prisms of adjacent layers decussate, and form bands known as Hunter-Schreger Bands (HSBs) (Fig. 1A) (Korvenkontio, 1934). The HSBs can be oriented in transverse, diagonal or longitudinal directions. Transversely arranged prisms are considered primitive and original, whereas longitudinally arranged prisms are considered the most advanced type (Kalthoff, 2000). The spatial arrangement of HSBs and orientation of IPM *vis* a *vis* the prisms are considered some of the most important features to evaluate the degree of development in rodent incisor enamel microstructure (Kalthoff, 2000). HSBs are considered to be strengthening devices and crack propagation inhibitors (the plywood effect) (Lehner and Plenck, 1936; Koenigswald and Pfretzschner, 1987, 1991; Pfretzschner 1988, 1994). The three-dimensional arrangement of different enamel types within a tooth defines its "Schmelzmuster" (Koenigswald, 1980).

Tomes (1850) identified two basic kinds of enamel structures by studying the arrangement of enamel prisms and Korvenkontio (1934) named these 'Uniserial' (one prism wide) and 'Multiserial' (three to seven prisms wide, Fig. 3B) and defined a third type 'Pauciserial' (two to six prism wide, Fig. 3A).

The fossil muroid rodent (murids- rats and mice; cricetids-hamsters; spalacids-bamboo rats, etc.) record is fairly rich and is distributed mainly along the foothills and some in the Kachchh basin of Gujarat. To date very few studies have been carried out on the taxonomy, phylogeny and biomechanics of fossil muroid rodents based on their incisor enamel microstructure. Therefore, in the present study, an attempt has been made to evaluate the incisor enamel microstructure of fossil muroid rodents for taxonomic, phylogenetic and biomechanical implications by comparing them with those of their extant counterparts.

MATERIALS AND METHODS

Bulk rock samples collected from different fossiliferous Neogene localities exposed around Ramnagar (J&K), Ghaggar River (Nadah Sahab and Khetpurali), Markanda River (Moginand, Kanthro and Devni Khadri of Himachal Pradesh), and Kachchh (Gujarat) were transported to the laboratory for maceration, followed by sorting of the rodent incisors. The rodent teeth recovered from various sites were tied to the composite stratigraphy of the area. The stratigraphic assignment of the muroid rodents from the Siwaliks was done by integrating the available locality data into the sections previously dated using magnetostratigraphy, tephrochronology and biostratigraphy.

Several recent owl pellets were collected in the field to extract modern rodent specimens to make a reference data set. The modern muroid rodents studied include *Mus musculus domesticus, M. m. musculus, M. m. tytleri, Mus booduga, Rattus rattus, Golunda ellioti, Nesokia indica, Millardia meltada, Bandicota indica, Gerbillus gleadowi* and *Tatera indica.* One incisor of a chapattimyid rodent collected from the Eocene sediments of Kalakot (J&K) was also studied for comparative analysis as these rodents have pauciserial HSBs (Sahni, 1980; Kumar *et al.,* 1997) (Fig. 3A).

The fossil rodent incisors were separated from all collected fossil samples. Before taking the photographs under Leica Stereo Zoom Microscope with scale, the samples were washed ultrasonically and dried under the lamp. Then they were embedded into an m-seal to make longitudinal and transverse sections (Fig. 4A & B). The sections were then ground and polished using 100, 400 and 800 mesh carborundum powder and etched with 5% HNO_3 for 10 to 15 seconds (according to the size of the sample). Samples were then mounted on SEM stubs with the help of double-side sticky tape and were coated with gold in a vacuum evaporator system (JEOL JFC-1600). The gold-coated samples were studied and photographed for ultrastructural analysis under JEOL JSM-25S Scanning Electron Microscope (SEM) housed at CAS in Geology, Panjab University, Chandigarh.

Abbreviations: VPL/AS- Vertebrate Palaeontology Laboratory/Ankita Singla, PU- Panjab University, R-Ramnagar, Ka-Kalakot, KU-Kachchh, M- Moginand, DK-Devni Khadri, K-Kanthro, MMT- *Mus musculus tytelri,* GE-*Golunda ellioti*

MEASUREMENTS

Transverse and sagittal sections were made to obtain several linear and angular measurements to identify the fossil incisors. Korvenkontio (1934) defined the "External Index" as the ratio between outer enamel thickness to total enamel thickness. Flynn (1977) defined the boundary between various layers where most of the rods bend from inner enamel to outer enamel. External Index is expressed in ratio form. The total enamel thickness varies depending on the cutting of the section, as a small tilt in the angle can cause SEM magnification error of up to 10%. Total enamel thickness varies within a species as well as between different species but the ratio of outer enamel to total enamel thickness is less variable and is considered a reliable parameter for identification. The external index can be significantly greater in immature incisors than in adult ones (Escala and Gallego, 1977).

Band width is another useful linear measurement defined by Korvenkontio (1934). In a sagittal section, band width is equal to the thickness of the rod in uniserial enamel (Fig. 1B). It must be measured perpendicular to the inclination because most bands are curved and may become thin near the dentine. Band width is calculated by averaging an even number of adjacent bands in the middle of inner enamel to avoid error (Flynn, 1977) (Fig. 1B).

Further, Korvenkontio (1934) defined two useful angular measurements, i.e., incisal inclination and outer enamel

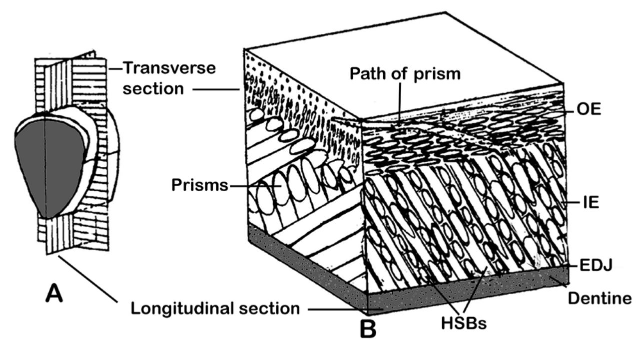

Fig. 4. Schematic diagram showing incisor sections. A. Transverse and longitudinal sections, B. Model of incisor enamel microstructure showing prism orientation and path of prisms from enamel-dentine junction to outer enamel surface. EDJ- Enamel-Dentine junction, HSB- Hunter-Schreger Bands, OE- Outer Enamel and IE- Inner Enamel (modified after Patnaik, 2002).

inclination. The incisal inclination is defined as the angle between a linear structure and a line normal to the enamel-dentine boundary (Fig. 1B). Structures with high inclination are nearly parallel to the boundary. In a sagittal section, bands of inner enamel are inclined, and the inclination is greater for lower incisors than for the upper incisors. As bands are curved, the incisal inclination is measured as a tangent to the curved band from the centre (Fig. 1B). Rods of the outer enamel has a high inclination. In the outer enamel, rods bend towards the tip of the incisor, so the angle is measured towards the tip of the incisor.

In transverse sections, the only useful parameter used for analyses is the "Decussation Angle". The prisms of adjacent rows are inclined and cross each other in the opposite direction known as decussation. The angle between these inclined prisms in the opposite direction is known as Decussation Angle and the angle between crossed prisms is open towards the surface and dentine (Fig.1A). The decussation angle increases from the enamel-dentine junction to the outer surface of the enamel.

A sagittal section is generally preferred over the transverse section to take measurements of enamel microstructure for several reasons. It is difficult to control the orientation of transverse sections and some transverse characters are repetitious. While it is easy to control the orientation of the sagittal section and measurements are easily observed. Measurements have been taken from the area around the midline of incisors rather than from the mesial and lateral edges.

SYSTEMATICS

Fossil incisor samples collected from various Siwalik and Kachchh localities are described and compared below.

Order **Rodentia** Bowdich, 1821
Family **Muridae** Illiger, 1811
Subfamily **Murinae** Illiger, 1811
Antemus **Jacobs**, 1977

cf. *Antemus*

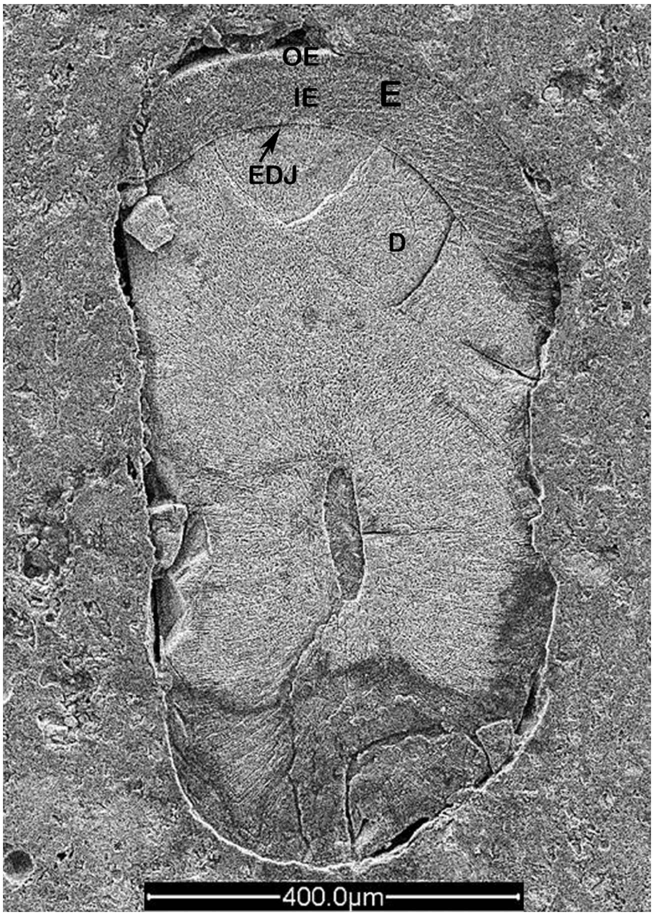

Fig. 5. SEM micrograph of rodent incisor (VPL/AS/R-1) from Ramnagar area showing semi-triangular cross-section. OE- Outer enamel, IE- Inner enamel, E- Enamel, D- Dentine, EDJ- Enamel- Dentine Junction.

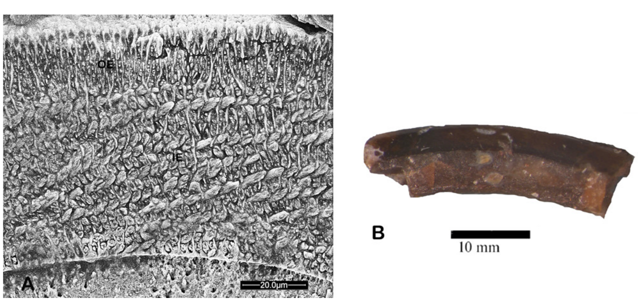

Fig. 6. A. SEM micrograph showing a transverse section of fossil incisor (VPL/AS/R-1) from Ramnagar area, B. Microscopic image of fossil incisor.

Locality and age: Ramnagar area, Lower Siwaliks (~13.2-13.8Ma, Middle Miocene).

Referred material: VPL/AS/R-1 and VPL/AS/R-5.

Description

External description of incisor enamel: The cross-section of incisor VPL/AS/R-1 oval (Fig. 5), surface smooth, lacking ridges or grooves, enamel colour brown and radius of curvature small (Fig. 6B).

The internal structure of incisor enamel: The incisor enamel of VPL/AS/R-5 istwo-layered with uniserial HSBs in PI and radial enamel in the PE (Fig. 7A), enamel thickness 84µm, PE occupies ~20%. HSBs are transversely arranged, moderately inclined at the centre and mesial side, diagonally arranged towards the lateral side of the inner enamel (Fig. 7A). Outer radial enamel, with parallel prism sand perpendicular IPM forms a mesh like structure (Fig. 7D). Modified radial enamel is present near the EDJ where inter-row sheets of IPM separates HSBs are aligned parallel to each other. In TS, prisms appear rounded to sub-rounded (Fig. 7C), decussate at high angles (80°-90°), IPM crystallites at angles to the prisms in the third dimension (Fig. 7C). In LS, incisal prism bands inclined at 10° in PI and 70° in the outer enamel, band width 4µm (Fig. 7B).

Comparisons: Middle Miocene deposits of Lower Siwaliks of Ramnagar area are rich in rodent fossils that include murine (*Antemus*), gerbilline (*Myocricetodon*), cricetine (*Megacricetodon*), rhizomyine (*Kanisamys*), sciurine (*Tamias*), and ctenodactyline (*Sayimys*) (Sehgal and Patnaik, 2012; Parmar *et al.,* 2018).

VPL/AS/R-1 and VPL/AS/R-5 differ from gerbillines because the latter show uniserial enamel microstructure with a grooved upper incisor enamel surface and a lower incisor with a small notch near its mesial end (Kalthoff, 2000; Patnaik, 2001). The present specimens differ from cricetid incisors in lacking ornamentation (ridges/grooves) on the enamel surface (Kalthoff, 2000, also see below). Further, these can be separated from the incisors of spalacids because the latter show three to four-layered advanced enamel structures with thicker outer enamel (>30%) and often with a ridge on the enamel surface. Moreover, rhizomyid incisors are much larger and have triangular cross-sections. Ctenodactylids show pauciserial to multiserial enamel microstructure (Martin, 1995).

VPL/AS/R-1 and VPL/AS/R-5 have almost similar enamel microstructure and are closely similar to those of murines because of the uniserial enamel type with smooth enamel surface and cross-section of these samples are oval. HSBs are transversely arranged in the centre and slightly diagonally arranged towards mesial and lateral end in the inner enamel. Both the samples show modified radial enamel near EDJ. Because of low incisal inclination (30°) in the longitudinal section and the presence of a high number of HSBs (approx. 30), both these samples are of lower incisors.

As incisor enamel microstructure of fossil samples VPL/AS/R-1 and VPL/AS/R-5 show very close resemblance to those of modern mice *Mus* (Fig. 1& 2), and no murine taxa other than *Antemus* has been found from Ramnagar area, therefore these fossil samples are referred here as cf. *Antemus.*

Progonomys Schaub, 1938

cf. *Progonomys*

Locality and age: Tapar, Kachchh (11-10 Ma, late Miocene).

Referred material: VPL/AS/KU-5, VPL/AS/KU-7, VPL/AS/KU-8, VPL/AS/KU-10, VPL/AS/KU-13 and VPL/AS/KU-14.

Description

External description of incisor enamel: VPL/AS/KU-5 (Fig. 8A and B) dark brown enamel with smooth surface.

Internal structure of enamel: The incisor enamel of VPL/AS/KU-5 is two-layered with uniserial HSBs in PI and radial enamel in PE (Fig. 9A), enamel thickness 100µm, PE occupies < 20% of total enamel thickness (Table-2). In TS, prisms are sub-rounded to oval, (Fig. 9A), decussate at 80° and IPM crystallites at an angle to prisms in the third dimension (Fig. 9A), transversely arranged HSBs moderately inclined at the centre and diagonally arranged towards the mesial and lateral ends of inner enamel, the outer enamel radial with parallel prisms and perpendicular IPM (Fig. 9A). In LS, incisal prism bands inclined at 40° in PI and 0° in outer enamel, band width 4µm (Fig.9B).

Comparison: Fossil incisor samples VPL/AS/KU-5, VPL/AS/KU-7, VPL/AS/KU-8, VPL/AS/KU-10, VPL/AS/KU-13 and VPL/AS/KU-14 have almost similar enamel microstructure but differ from those of the cricetids in having smooth enamel surface and lack of any surface ornamentation or wrinkles. Gerbillines differ in having a sulcus and notch in lower incisors towards the mesial end. Rhizomyines have three- to four-layered enamel and ctenodactylids show pauciserisal to multiserial enamel microstructure. The present specimens can be safely placed under murines because of almost similar incisor enamel microstructure, smooth enamel surface, oval-shaped cross-section and smaller size. All the samples have high incisal inclination and the presence of higher number of HSBs and are therefore lower incisors.

Enamel microstructure of fossil incisors VPL/AS/KU-5, VPL/AS/KU-7, VPL/AS/KU-8, VPL/AS/KU-10, VPL/AS/KU-13 and VPL/AS/KU-14 is very similar to that of *Progonomys* studied by Kalthoff (2000). Bhandari *et al.*, (2021) reported *Progonomys morganae* from the late Miocene of Tapar in Kachchh area. *Progonomys* is considered as an ancestral form of *Mus* (Jacobs, 1978). Therefore, the aforementioned fossil samples are referred to here as cf. *Progonomys*.

Bandicota Gray, 1873 and ***Nesokia*** Gray, 1842

cf. *Bandicota* or cf. *Nesokia*

Locality and age: Moginand, Upper Siwaliks (~ 4-3.5 Ma, Early Pliocene); Devni Khadri, Upper Siwaliks (~3Ma, Late Pliocene).

Referred material: VPL/AS/M-1, VPL/AS/M-4 and VPL/AS/DK-1.

Internal structure of enamel- The enamel of VPL/AS/M-1 two-layered, uniserial HSBs in PI and radial enamel in PE (Fig. 11A), total enamel thickness 106µm, PE occupies 30%. In TS, prisms sub-rounded to oval (Fig. 11A) and decussate at 60°–70° (Decussation angle increases from enamel-dentine junction towards the outer enamel surface) and IPM crystallites at an angle to prisms in the third dimension (Fig. 11A). The transversely arranged HSBs are moderately inclined in inner enamel and outer enamel is radial with parallel prisms and perpendicular IPM (Fig. 11A). In LS, incisal prism bands inclined at 30° in PI and at 70° in outer enamel and band width 3µm (Fig. 11B) (also see, Table- 3), incisor cross-section sub-triangular (Fig. 10).

External description of enamel- The incisor enamel of VPL/AS/DK-1 is light to dark brown, with a shallow groove/depression on the surface of the enamel (Fig. 12B). Cross-sectional view sub-triangular (Fig. 12A).

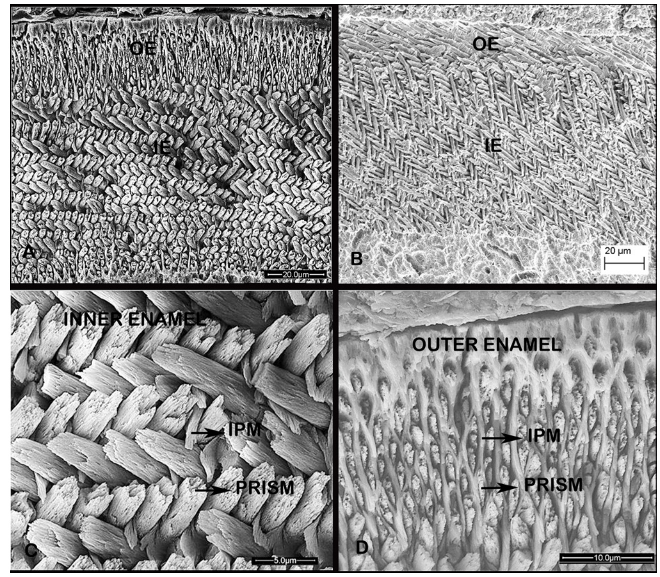

Fig. 7. SEM micrographs of fossil incisor (VPL/AS/R-5) from Ramnagar area showing, A. Transverse section, B. Longitudinal section, C. Magnified image of inner enamel showing IPM and prism orientation, D. Magnified image of outer radial enamel showing mesh-like structure. OE- Outer enamel, IE- Inner enamel, IPM- Inter- Prismatic Matrix.

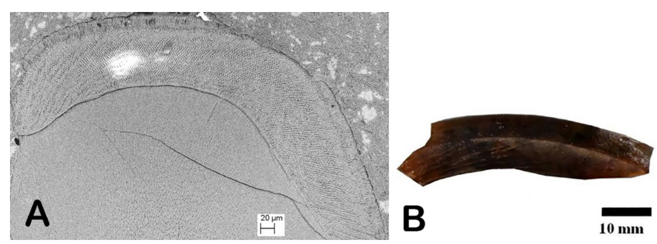

Fig. 8. A. SEM micrograph of fossil incisor VPL/AS/KU-5 from Kachchh area showing enamel and dentine in cross-section, B. Microscopic image of fossil incisor showing its side view with the smooth enamel surface.

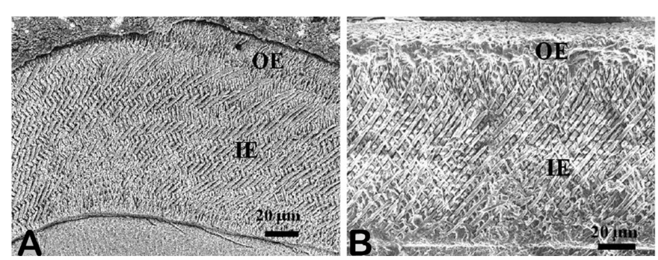

Fig. 9. SEM micrographs of fossil incisor VPL/AS/KU-5 from Kachchh area showing A. Transverse section, B. Longitudinal section.

Internal structure of the enamel- Incisor of VPL/AS/DK-1 two-layered with uniserial HSBs in PI and radial enamel in PE (Fig.13A), total enamel thickness 120µm, PE occupies almost 25% (Table- 4). In TS, prisms are oval to flattened (Fig. 13A), decussate at 90° and IPM crystallites at an angle to prisms in the third dimension (Fig. 13A). The transversely arranged HSBs are moderately inclined in inner enamel and in outer enamel prisms parallel with perpendicular IPM forming a net-like structure (Fig. 13A). In LS, incisal prism bands inclined at 30° in PI and 70° in outer

Table-1. Linear and angular measurements of enamel microstructure of fossil incisors of Ramnagar area (Middle Miocene).

SPECIMEN NUMBER	INCISOR CROSS-SECTION	TE (μm)	EI	II(°)	OI(°)	BW	α(°)	IPM INCLINATION	HSB ORIENTATION	PRISM CROSS SECTION IN PI	MODIFIED RADIAL ENAMEL	ENAMEL SURFACE
VPL/AS/R1	Oval	76	0.19	30	95	3	80-90	angled	Transverse & slightly diagonal	Round	present	Smooth
VPL/AS/R2	Oval	89	0.21					IPI-angled OPI-parallel	IPI-transverse OPI-longitudinal	Flattened	absent	Ridge
VPL/AS/R3	Oval	104	0.18	45		3.5	80-90	angled	Transverse & slightly diagonal	Round	absent	2 Longitudinal ribs
VPL/AS/R4	Oval	120	0.20				90	angled	transverse	Round	present	2 Longitudinal ribs
VPL/AS/R5	Oval	84	0.21	10	70	4	80-90	angled	Transverse & slightly diagonal	Round	present	Smooth
VPL/AS/R6	Triangular?	75	0.34					IPI-angled OPI-parallel	IPI-transverse OPI-longitudinal	Oval to Flattened	absent	Ridge
VPL/AS/R7	Oval	120	0.22				70-80	angled	diagonal	Oval to Flattened	absent	2 Longitudinal ribs

Table-2. Linear and angular measurements of enamel microstructure of fossil incisors Kachchhfrom Kachchh area (Late Miocene).

SPECIMEN NUMBER	INCISOR CROSS-SECTION	TE (μm)	EI	II(°)	OI(°)	BW (μm)	α(°)	IPM INCLINATION	HSB ORIENTATION	PRISM CROSS SECTION IN PI	MODIFIED RADIAL ENAMEL	ENAMEL SURFACE
VPL/AS/KU-2	Round oval	77	0.25	45			~90	IPI- angled OPI-parallel	IPI- transverse OPI-longitudinal	Sub-round to oval	absent	Longitudinal Ridge
VPL/AS/KU-5	Round oval	100	0.17	40	70	4	80	angled	Transverse & diagonal (mesial & lateral)	Sub-round to oval	absent	Smooth surface
VPL/AS/KU-7	Round oval	136	0.14	35	80	3	70	angled	Transverse & diagonal (mesial & lateral)	Round to sub-round	absent	Smooth surface
VPL/AS/KU-8	oval	102	0.16	40	80	3	80	angled	Transverse & diagonal (mesial & lateral)	Round to Sub-round	absent	Smooth surface
VPL/AS/KU-10	Oval	113	0.17	35	95	3	60	angled	transverse	Sub-round to oval	absent	Smooth surface
VPL/AS/KU-11	Round oval	97	0.22	20	80	3	70	angled	transverse	Sub-round to oval	absent	Smooth surface
VPL/AS/KU-12	Oval	100	0.22	20	80	3.5	90	angled	transverse	Oval to flattened	absent	Smooth surface
VPL/AS/KU-13	Oval	111	0.15	10		3.5	80	angled	transverse	Oval to flattened	absent	Smooth surface
VPL/AS/KU-14	Oval	100	0.27	20	80	3	80	angled	transverse	Sub-round to oval	absent	Smooth surface
VPL/AS/KU-16		191	0.15	40	100	20		angled	multiserial	oval	absent	Smooth surface
VPL/AS/KU-17	Round oval	107	0.33	10	50	4	90	parallel	transverse	Oval to flattened	absent	Smooth surface

enamel, band width 3μm (Fig. 13B), a thin layer of modified radial enamel near EDJ.

Comparison: Fossil samples VPL/AS/M-1 and VPL/AS/M-4 have almost similar enamel microstructure but differ from those of Cricetidae and Gerbillinae in the absence of surface ornamentation. They do not show any relationship to the Ctenodactylidae because of having uniserial enamel structure. The fossil samples VPL/AS/M-1 and VPL/AS/M-4 are closely similar to the incisor enamel microstructure with extant murine species *Bandicota indica* and *Nesokia indica*

Table-3. Linear and angular measurements of enamel microstructure of fossil incisors of Moginand area (Early Pliocene).

SPECIMEN NUMBER	INCISOR CROSS-SECTION	TE (µm)	EI	II(°)	OI(°)	BW (µm)	α(°)	IPM INCLINATION	HSB ORIENTATION	PRISM CROSS SECTION IN PI	MODIFIED RADIAL ENAMEL	ENAMEL SURFACE
VPL/AS/M-1	Sub-triangular	106	0.28	30	70	3	60-70	Angled	Transverse HSB	Sub-round to oval	absent	Smooth
VPL/AS/M-2		137	0.20	30	85	3	50	Angled	Transverse (centre) and diagonal (mesial and lateral end)	Oval to flattened	absent	grooved
VPL/AS/M-4		83	0.40	60	70	2.5	70	Angled	Diagonal HSB	Sub-round to oval	absent	Smooth
VPL/AS/M-5		94	0.25	20	60	2.5	90	Angled	Transverse HSB	Round to flattened	absent	Sulcus
VPL/AS/M-6	Oval shaped	149	0.28	40	70	2	90	Angled	Transverse HSB	Sub-round to oval	Absent	Smooth
VPL/AS/M-7	Sub-triangular	115	0.16	45	90		50	Angled	Transverse HSB	Sub-round to oval	absent	Smooth
VPL/AS/M-8	Sub-triangular	150	0.15	50			90	Angled	Transverse HSB	Sub-round to oval	present	Smooth
VPL/AS/M-10	Oval shaped	125	0.19				90	Angled	Transverse HSB	Sub-round to oval	absent	Smooth
VPL/AS/M-11	Sub-triangular	137	0.17	45	70	3	60	Angled	Transverse HSB	Sub-round to oval	absent	Smooth
VPL/AS/M-13	Sub-triangular	103	0.21	25	50	3		Angled	Transverse (centre) and diagonal (mesial and lateral end)	Sub-round to oval	absent	Smooth
VPL/AS/M-15	Sub-triangular	132	0.25	5	60	5	70	Angled	Diagonal	Oval to flattened	absent	Smooth
VPL/AS/M-16	Sub-triangular	127	0.19	50	80	3	70	Angled	Transverse	Oval to flattened	absent	Smooth
VPL/AS/M-18	Sub-triangular	128	0.17	50	85		70	Angled	transverse	oval	absent	Smooth
VPL/AS/M-19	Oval	122	0.22	20	70	4	80	Angled	Transverse (centre) and diagonal (mesial and lateral end)	Oval to flattened	Absent	Smooth
VPL/AS/M-20	Sub-triangular	115	0.27	50	70	14		IPI-angled OPI-parallel	IPI-Transverse OPI- longitudinal	Oval to flattened	Absent	Smooth

Table-4. Linear and angular measurements of enamel microstructure of fossil incisors of Devni Khadri area (Late Pliocene).

SPECIMEN NUMBER	INCISOR CROSS-SECTION	TE (µm)	EI	II(°)	OI(°)	BW (µm)	α(°)	IPM INCLINATION	HSB ORIENTATION	PRISM CROSS SECTION IN PI	MODIFIED RADIAL ENAMEL	ENAMEL SURFACE
VPL/AS/DK-1	Sub-triangular	120	0.24	30	70	3	90	angled	Transverse HSB	Oval to flattened	Absent	Slightly wrinkled
VPL/AS/DK-2	Oval	76	0.36	25	65	4	60	angled	Transverse HSB	Oval to flattened	absent	smooth
VPL/AS/DK-3	Oval	55	0.41				80	angled	Transverse HSB	Oval to flattened	Absent	Smooth
VPL/AS/DK-12	Oval	113	0.15	50	90	3	60	angled	Transverse (centre) and diagonal (lateral)	Oval to flattened	Absent	Smooth

in having sub-triangular cross-section (Fig. 10), thick OE and gentle band inclinations.

VPL/AS/DK-1 has a sub-triangular cross-section and a lightly-wrinkled enamel surface (Fig. 12A&B). Its enamel microstructure is comparable to that of extant murine species *Bandicota*/*Nesokia* in sub-triangular cross-section, thick OE and gentle band inclinations.

As a cross-section of the incisor is one criterion used in this research to separate between *Mus* and *Karnimata* (late Miocene Murine) lineages, the present specimens can be placed under *Karnimata* lineage for having a sub-triangular cross-section. The fossil incisor samples VPL/AS/M-1, VPL/

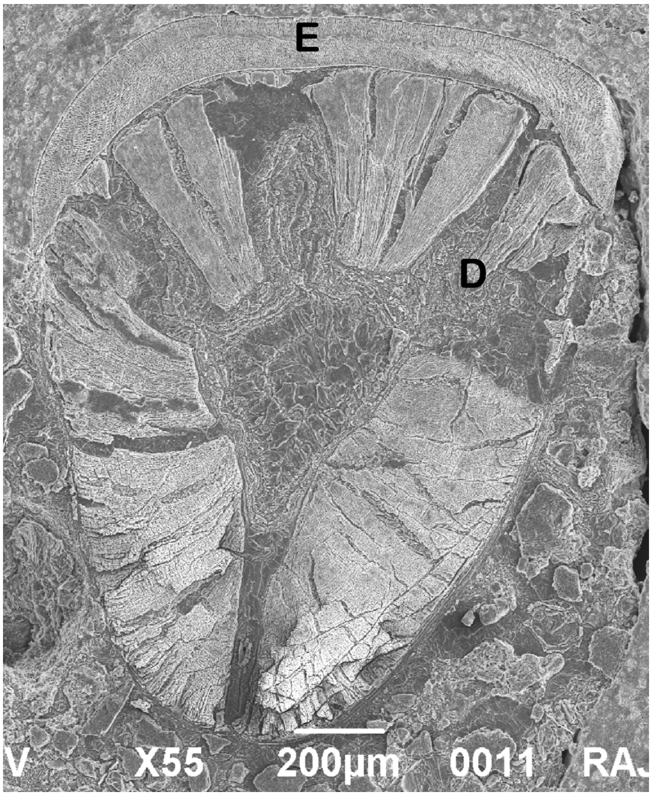

Fig. 10. SEM micrograph of fossil incisor VPL/AS/M-1 from Moginand area showing sub-triangular cross-sectional view.

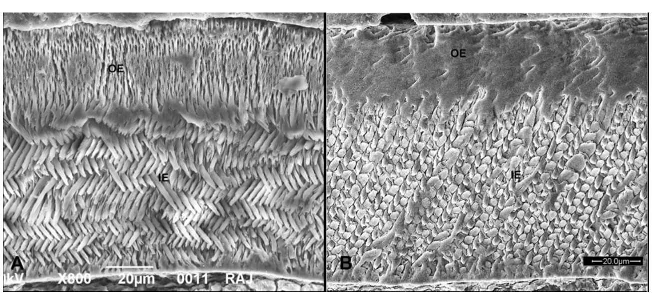

Fig. 11. SEM micrographs of fossil incisor VPL/AS/M-1 from Moginand area showing A. Transverse section, B. Longitudinal section.

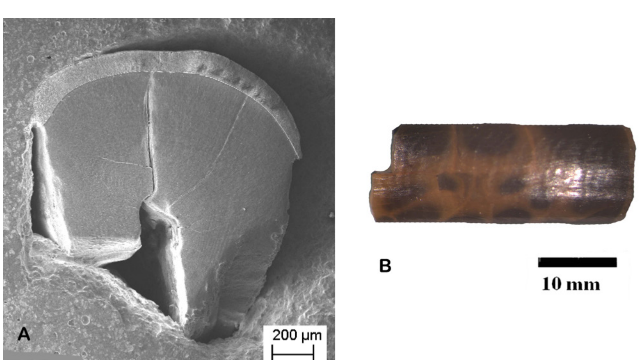

Fig. 12. A. SEM micrograph of fossil incisor VPL/AS/DK-1 from Devni Khadri area showing enamel and dentine in cross-section, B. Microscopic image showing top view of fossil incisor with a shallow depression on the enamel surface.

AS/M-4 and VPL/AS/DK-1can be assigned either to cf. *Bandicota* or *Nesokia* as it is difficult to differentiate between the two based on enamel microstructure.

Millardia Thomas, 1911

cf. *Millardia*

Locality and age: Moginand, Upper Siwaliks (~ 4-3.5 Ma, Early Pliocene).

Referred material: VPL/AS/M-7, VPL/AS/M-8, VPL/AS/M-11, VPL/AS/M-13, VPL/AS/M-16 and VPL/AS/M-18.

Internal structure of enamel- Incisor of VPL/AS/M-11 two-layered with uniserial HSBs in PI and radial enamel in PE (Fig. 14), total enamel thickness is137µm, PE occupies < 20% (Table- 3). In TS, prisms sub-rounded to oval (Fig. 15A) decussate at 60° and IPM crystallites at an angle to the prisms (Fig. 15A), transversely arranged HSBs steeply inclined in inner enamel and outer enamel radial with parallel prisms and perpendicular IPM (Fig. 15A). In LS, incisal prism bands inclined at 45° in PI and at 70° in outer enamel and band width 3µm (Fig. 15B), incisor cross-section sub-triangular (Fig. 14).

Comparison: Fossil incisor samples VPL/AS/M-7, VPL/AS/M-8, VPL/AS/M-11, VPL/AS/M-13, VPL/AS/M-16, and VPL/AS/M-18 have HSBs that are transverse to diagonally arranged with angled IPM and outer radial enamel with sub-triangular cross-section and smooth enamel surface. These samples do not show any affinity to those of cricetine and gerbilline because of the absence of surface ornamentation. Nor can they be assigned to ctenodactylid. These are related to *Karnimata* lineage because of having a sub-triangular cross-section and bigger size than *Mus.* However, the incisor enamel microstructure of these fossil samples is almost similar to that of the extant murine genus *Millardia.* Therefore, all of the aforementioned samples are assigned to cf. *Millardia.*

Mus Clerck, 1757

cf. *Mus*

Locality and age: Moginand, Upper Siwaliks (~ 4- 3.5 Ma- Early Pliocene); Devni Khadri, Upper Siwaliks (~3Ma, Late Pliocene); Kanthro, Upper Siwaliks (~ 3Ma, Late Pliocene).

Referred material: VPL/AS/M-6, VPL/AS/M-10 and VPL/AS/M-19, VPL/AS/DK-2, VPL/AS/DK-3 and VPL/AS/DK-12, VPL/AS/K-1, VPL/AS/K-2, VPL/AS/K-4, VPL/AS/K-6, VPL/AS/K-7, and VPL/AS/K-8.

Internal structure of enamel- Internal enamel microstructure of VPL/AS/M-6 is two-layered with uniserial HSBs in PI and radial enamel in PE (Fig. 17A), enamel thickness 149µm, PE <30%. In TS, prisms are sub-rounded to oval and decussate at 90° and crystallites of IPM at an angle to the prisms in the third dimension (Fig. 17A). The transversely arranged HSBs are steeply inclined in the inner enamel and the outer enamel is radial with parallel prisms and perpendicular IPM (Fig. 17A). In LS, incisal prism bands inclined at 40° in PI and 70° in the outer enamel, band width 2µm (Fig. 17B), CS oval (Fig. 16).

External description of enamel- VPL/AS/DK-2 oval in CS (Fig. 18A) and dark brown (Fig. 18B).

Internal structure of enamel- Devni Khadri incisor two-layered with uniserial HSBs in PI and radial enamel in PE (Fig. 19A), enamel thickness 76µm, PE 36% (Table- 4). In TS, prisms are oval to flat (Fig. 19A) and decussate at 60° and the IPM crystallites at an angle to the prisms in the third dimension (Fig.19A). Transversely arranged HSBs steeply inclined in the inner enamel and outer enamel prisms are parallel with perpendicular IPM forming a net-like structure (Fig. 19A). In LS, incisal prism bands inclined at 25° in PI and 65° in outer enamel and band width 4µm (Fig. 19B).

External description of enamel- VPL/AS/K-4 (Fig. 20A) is oval in cross-section and dark brown (Fig. 20B).

Internal structure of enamel- VPL/AS/K-4 two-layered with uniserial HSBs in the PI and radial enamel in the PE (Fig. 21A). Total enamel thickness is 109µm, PE 20% (Table-4). In TS, prisms are sub-rounded to oval and decussate at 80° and the crystallites of IPM at an angle to the prisms in the third dimension (Fig. 21A). Transversely arranged HSBs are steeply inclined in the inner enamel and in the outer enamel prisms are parallel with perpendicular IPM forming a net-like structure (Fig. 21A). In the LS, incisal prism bands are inclined at 50° in PI and 70° in the outer enamel and the band width is 2.5µm (Fig. 21B).

Comparison: Fossil samples VPL/AS/M-6, VPL/AS/M-10 and VPL/AS/M-19 appear oval in cross-sections, have smooth enamel surfaces and uniserial enamel. In contrast, Cricetidae and Gerbillinae incisors have surface ornamentation and Ctenodactylidae have either pauciserial or multiserial type structure. All the aforementioned incisors show similarity to the *Mus* lineage because of the oval-shaped cross-section, smooth enamel surface and uniserial enamel with transverse HSBs and angled IPM and outer radial enamel.

VPL/AS/DK-2, VPL/AS/DK-3 and VPL/AS/DK-12 show smooth enamel surface and oval-shaped cross-sections. All the fossil samples are very similar to the *Mus* lineage because of having smooth enamel surface, oval-shaped cross-section, uniserial enamel with transversely aligned HSBs and angled IPM and radial outer enamel.

VPL/AS/K-1, VPL/AS/K-2, VPL/AS/K-4, VPL/AS/K-6, VPL/AS/K-7, and VPL/AS/K-8 differ from gerbillines and cricetids in having smooth enamel surface and from spalacids in having two-layered enamel microstructure. All these samples are mostly similar to murines in having smooth enamel surface, oval to sub-triangular shaped cross-sections, uniserial enamel structure with transverse to diagonal HSBs and outer radial enamel. All of the aforementioned samples are placed here under cf. *Mus*.

Golunda Gray, 1837

cf. *Golunda*

Locality and age: Moginand, Upper Siwaliks (~ 4- 3.5 Ma- Early Pliocene); Kanthro, Upper Siwaliks (~ 3Ma, Late Pliocene).

Referred material: VPL/AS/M-2 and VPL/AS/K-3.

External description of enamel- VPL/AS/K-3 dark brown colour, with central groove on enamel surface (Fig. 22B). The cross-section is semi-triangular (Fig. 22A).

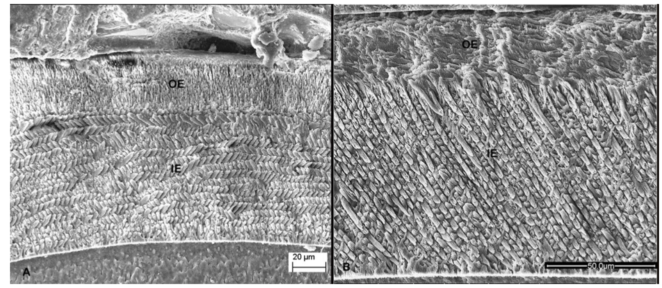

Fig. 13. SEM micrographs of fossil incisor VPL/AS/DK-1 from Devni Khadri area showing A. Transverse section, B. Longitudinal section (Scale-50µm).

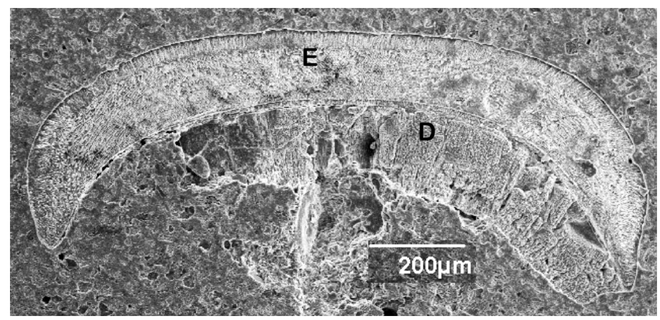

Fig. 14. SEM micrograph of fossil incisor VPL/AS/M-11 from Moginand area showing enamel and dentine microstructure and sub-triangular cross-sectional view. E- Enamel, D- Dentine.

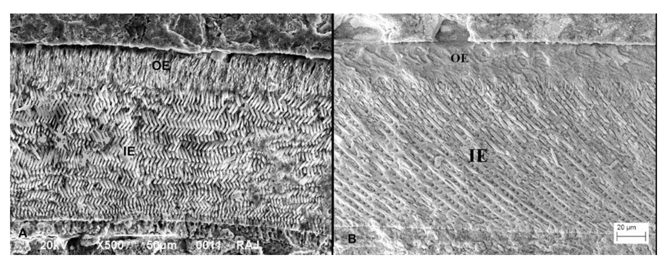

Fig. 15. SEM micrographs of fossil incisor VPL/AS/M-11 from Moginand area showing A. Transverse section, B. Longitudinal section.

Internal structure of enamel- VPL/AS/K-3 two-layered with uniserial enamel, outer enamel radial with parallel prisms and perpendicular IPM, groove present in the centre running parallel to the longitudinal axis, (Fig. 23A) divides the enamel into three parts- central part where the enamel is thin and outer two ridges where the enamel is thick (Fig. 23A). Inner enamel with transversely arranged HSBs with perpendicular IPM at the centre and diagonally arranged HSBs towards the lateral and mesial side (Fig. 23A). Enamel is 64µm thick and PE 20% of total enamel thickness (Table-5). In TS, prisms are oval to flat in CS and decussate at 60° and IPM crystallites at an angle to the prisms in the third dimension (Fig. 23A). In LS, incisal bands are inclined at 20° in PI and in outer enamel prisms are inclined at 45° (Fig. 23B). The band width is 5µm.

Internal structure of enamel- VPL/AS/M-2 two-layered uniserial enamel, outer enamel radial with parallel prisms and perpendicular IPM. A groove present in the centre (Fig. 24), HSBs with angled IPM in the centre and diagonally

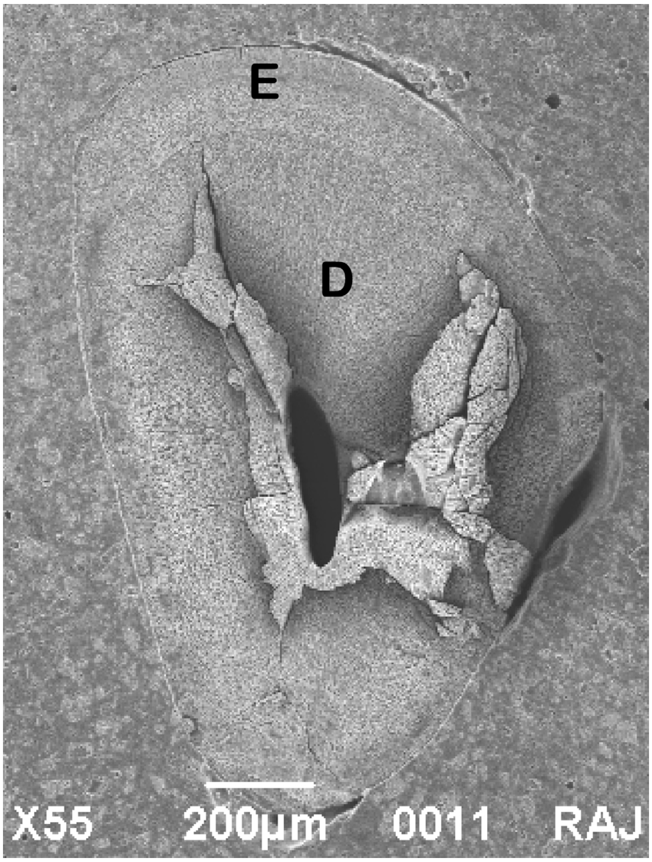

Fig. 16. SEM micrograph of fossil incisor VPL/AS/M-6 from Moginand area showing oval shaped cross-section.

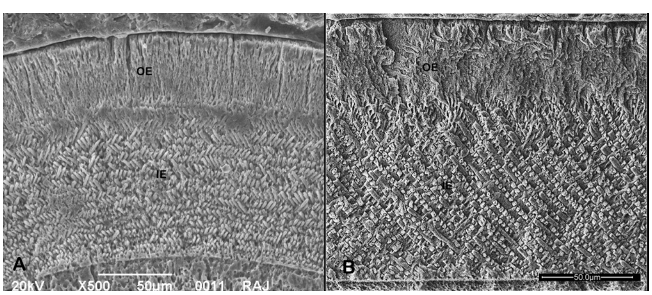

Fig. 17. SEM micrographs of fossil incisor VPL/AS/M-6 from Moginand area showing A. Transverse section, B. Longitudinal section.

arranged HSBs towards lateral and mesial sides (Fig. 25A). Enamel is 137μm thick and PE is 20% of total enamel thickness (Table- 3). In TS, prisms are oval to flat in CS and decussate at 50° (Fig. 25A) and IPM crystallites at a right angle (approximately) to the prisms in the third dimension (Fig. 25A). In LS, incisal bands are inclined at 30° in PI and outer enamel prisms inclined at 85°, band width of 3μm.

Comparison: The enamel microstructure of VPL/AS/M-2 is similar to that of extant *Golunda* and *Golunda kelleri* and *G. tatroticus* reported by Patnaik (2002). In *Golunda* the incisor enamel surface is grooved, with uniserial enamel type, transverse HSBs at the centre and diagonal HSBs towards the lateral and mesial ends with angled IPM and outer radial enamel.

VPL/AS/K-3 is almost similar to the extant species of *Golunda* discussed above and with sample VPL/AS/M-2 from Moginand area but differs in position of groove on the enamel surface. VPL/AS/K-3 is not related to gerbillines because of the difference in groove/sulcus structure and also not related to cricetids and *Mus* because of the presence of grooved enamel surface. Therefore, these two fossil samples are here referred to as cf. *Golunda.*

Subfamily **Gerbillinae** Gray, 1825
Abudhabia **de Bruijn** and Whybrow, 1994

cf. *Abudhabia*

Locality and age: Moginand, Upper Siwaliks (~ 4- 3.5 Ma- Early Pliocene)

Referred material: VPL/AS/M-5.

The internal structure of enamel- VPL/AS/M-5 two-layered uniserial type enamel, outer enamel radial with parallel prisms and perpendicular IPM. A wide sulcus is present at the centre running parallel to the longitudinal axis of the tooth (Fig. 26). Inner enamel with moderately inclined transversely arranged HSBs with perpendicular IPM in the centre (Fig. 27A). Enamel 94μm thick and PE 25% of total enamel thickness. In TS, prisms are rounded to flat in CS and decussate at 90° (Fig. 27A) and the crystallites of IPM are at an angle to the prisms in the third dimension (Fig. 27A). In LS, incisal bands are inclined at 20° in PI and the outer enamel prisms are inclined at 60° (Fig. 27B). Band width 2.5μm (Table-3).

Comparison: Fossil incisor VPL/AS/M-5 differs from those of cricetids as the latter has ribs on the surface. Murines do not show the presence of sulcus and rhizomyines have three-four layered uniserial enamel structure, unlike the present specimen. VPL/AS/M-5 is comparable to *Gerbillus* (Kalthoff, 2000) in the presence of a wide sulcus running parallel to the longitudinal axis of the tooth.

However, VPL/AS/M-5 shows enamel microstructural features that are closely similar to those of *Abudhabia* reported from the Moginand locality (see Kalthoff, 2000; Patnaik 2003). Therefore, this specimen is referred to as cf. *Abudhabia.*

Family **Cricetidae** Fischer von Waldheim, 1817
Subfamily **Cricetinae** Fischer de Waldheim, 1817
Democricetodon **Fahlbusch**, 1969

cf. *Democricetodon*

Locality and age: Ramnagar area, Lower Siwaliks (~13.2-13.8Ma, Middle Miocene).

Referred material: VPL/AS/ R-3, VPL/AS/ R-4, VPL/ AS/ R-7.

External description of enamel- Fossil incisor dark brown, tip well preserved (Fig. 28B), two ribs on the enamel surface of VPL/AS/R-3 (Fig. 28A).

Internal structure of enamel- Incisor sample VPL/AS/R-4 two-layered uniserial enamel with HSBs in PI and radial enamel in PE (Fig. 28 & 29). The total enamel thickness is 120μm, of which PE 20%. The transversely oriented HSBs are steeply inclined with angled IPM. In TS, prisms rounded to sub-rounded (Fig. 29B) and decussate at high angles (80°-

90°) (Fig. 29B). Two small but pronounced ribs are present on the enamel surface- one at the centre and the other towards the lateral side (Fig. 29A).

Comparisons: The specimens VPL/AS/R-3, VPL/AS/R-4 and VPL/AS/R-7 cannot be referred to gerbillinae because the latter shows a grooved upper incisor and a notch towards the mesial end in the lower incisors. Further, these samples differ clearly from rhizomyid incisors which have three-four layered enamel microstructure. As mentioned earlier ctenodactylids show Pauciserial to Multiserial enamel types and murines have smooth enamel surfaces, unlike the present specimens. VPL/AS/R-3, VPL/AS/R-4 and VPL/AS/R-7 can be referred to as three different species of cricetids as the position and size of ribs are different in all three samples. From Ramnagar area, a few taxa of cricetids were reported, such as *Megacricetodon daamsi, M. sivalensis, Punjabemys downsi*, *P. micros* and *Democricetodon* sp. (Sehgal and Patnaik, 2012; Parmar *et al.,* 2015, Parmar *et al.,* 2017; Parmar *et al.,* 2018; Singh *et al*., 2018). Flynn *et al.,* (1985) reported species of *Democricetodon* with two parallel enamel ribs. *Democricetodon* is characterised by the presence of more or less pronounced longitudinally running ribs on the enamel surface with diagonally arranged HSBs in the inner enamel and outer radial enamel (Kalthoff, 2000). *Megacricetodon* has a smooth enamel surface with outer radial enamel and inner decussating transversely oriented HSBs with angled IPM (Kalthoff, 2000). Incisor enamel microstructure of *Punjabemys* has not been studied yet. All the presently studied specimens can be referred as cf. *Democricetodon* because of close similarities in enamel microstructure with that of *Democricetodon*.

Family **Spalacidae** Gray, 1821
Subfamily **Rhizomyinae** Winge, 1887
Kanisamys **sp.** Wood, 1937

cf. *Kanisamys*

Locality and age: Ramnagar area, J&K (~13.2-13.8Ma, Middle Miocene); Tapar, Kachchh (11-10 Ma, late Miocene)

Referred material: VPL/AS/R-2, VPL/AS/ R-6, VPL/AS/ KU-2.

External description of incisor enamel: VPL/AS/R-6 brown in colour (Fig. 30B).

Internal structure of enamel: VPL/AS/ R-6 four-layered uniserial HSBs in PI and radial enamel in PE (Fig. 30C). Enamel 75µm thick and PE 35% of total enamel thickness. In TS, prisms oval to flat (Table-1). The inner enamel is divisible in two parts- inner portio interna (IPI) and outer portio interna (OPI). In IPI, HSBs are transversely arranged with angled IPM, OPI, HSBs are longitudinally arranged with parallel IPM. Outer enamel is divided into two layers- outer portio externa (OPE) and inner portio externa (IPE). OPE with parallel prisms, and parallel IPM, whereas IPE consists of tangential enamel. In LS, prisms decussate with IPM in the third dimension (Fig. 30C). A small ridge formed due to the thickening of the outer enamel and prisms of inner enamel arranged transversely (Fig. 30A). A four-layered enamel micro structure is considered a very advanced form of enamel type (Kalthoff, 2000).

External description of incisor enamel: Fossil incisor sample VPL/AS/ KU-2 shows both enamel and dentine in

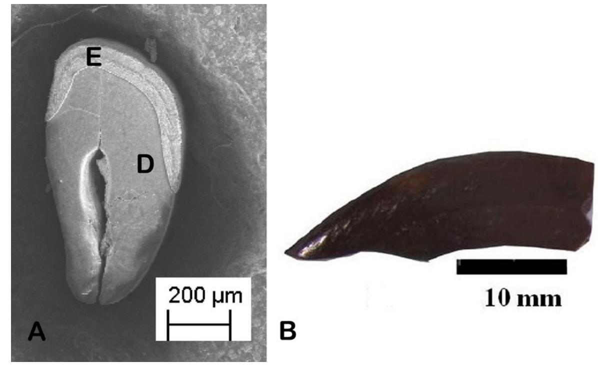

Fig. 18. A. SEM micrograph of fossil incisor VPL/AS/DK-2 from Devni Khadri area showing enamel and dentine in cross-section, B. Microscopic image of fossil incisor in side view showing smooth enamel surface. E- Enamel, D- Dentine.

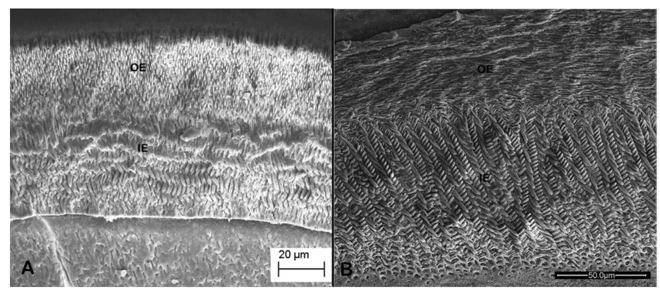

Fig. 19. SEM micrographs of fossil incisor VPL/AS/DK-2 from Devni Khadri area showing A. Transverse section, B. Longitudinal section (Scale- 50µm).

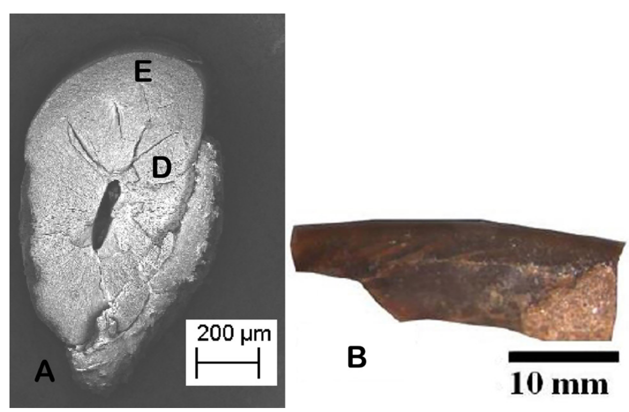

Fig. 20. SEM micrograph of fossil incisor VPL/AS/K-4 from Kanthro area showing, A. Enamel and dentine in the oval shaped cross-section, B. Microscopic image of fossil incisor in side view showing smooth enamel surface.

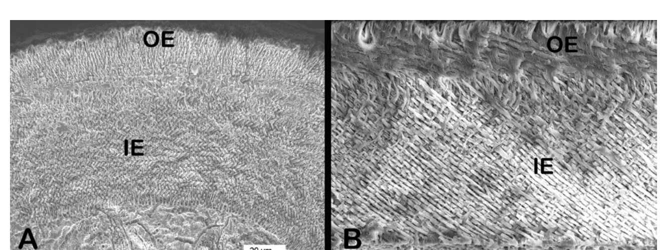

Fig. 21. SEM micrographs of fossil incisor VPL/AS/K-4 from Kanthro area showing A. Transverse section, B. Longitudinal section (Scale- 20µm).

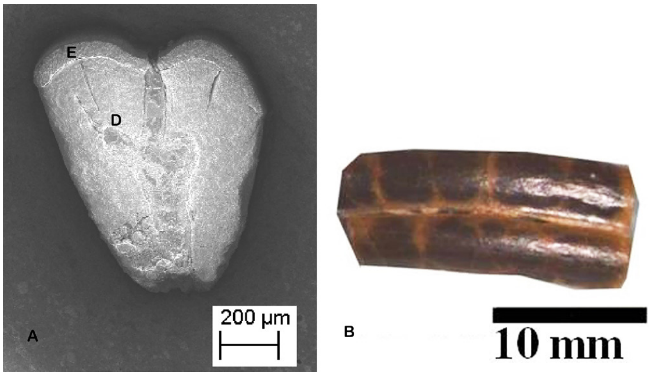

Fig. 22. SEM micrograph of fossil incisor VPL/AS/K-3 from Kanthro area showing, A. Enamel and dentine in the sub-triangular cross-section, B. Microscopic image showing side view of incisor with central groove on the enamel surface. E- Enamel, D- Dentine.

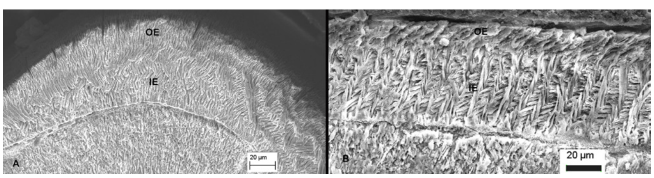

Fig. 23. SEM micrographs of fossil incisor VPL/AS/K-3 from Kanthro area showing A. Transverse section, B. Longitudinal section (Scale- 20µm).

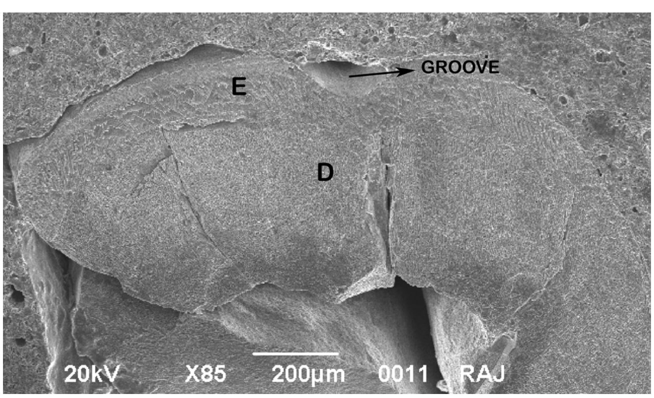

Fig. 24. SEM micrograph of fossil incisor VPL/AS/M-2 from Moginand area showing central groove with enamel (E) and dentine (D).

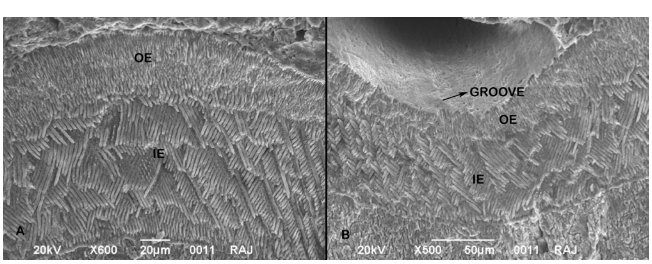

Fig. 25. SEM micrographs of fossil incisor VPL/AS/M-2 from Moginand area showing outer enamel (OE) and inner enamel (IE) A. Transverse section of ridge area and B. Transverse section of the grooved area.

the cross-section of the fossil incisor (Fig. 31A) and is dark brown with a smooth surface (Fig. 31B).

Internal structure of enamel: VPL/AS/ KU-2 three-layered uniserial enamel with HSBs in PI and radial enamel in PE (Fig. 32A). Enamel 77µm thick and PE is 25% of total enamel thickness (Table-2). In TS, prisms are sub-rounded to oval in CS. The inner enamel divided into two parts- inner portio interna (IPI) and outer portio interna (OPI) . In thin IPI, HSBs are transversely arranged with angled IPM and in thick OPI, HSBs are longitudinally arranged with parallel IPM. Outer enamel radial with parallel prisms and perpendicular IPM (Fig. 32A). A small ridge is formed due to the thickening of the outer enamel and here prisms of inner enamel are arranged transversely (Fig. 32A). In LS, HSBs decussate at 45° with angled IPM in the third dimension (Fig. 32B). A three-layered enamel microstructure is considered to be an advanced form of enamel type (Kalthoff, 2000).

*Comparison***:** VPL/AS/R-2 and VPL/AS/R-6 differ from gerbilline, cricetine, ctenodactyline and murine in having four-layered uniserial enamel structure. Fossil samples are similar to those of rhizomyines in having three (VPL/AS/R-2) to four (VPL/AS/R-6) layered structures and thicker outer enamel with a ridge, where longitudinal HSBs become transversely oriented (Kalthoff, 2000). The cross-section of incisors is triangular and fossil samples are larger. Rhizomyine in the Ramnagar area is represented by two species, *Kanisamys indicus* and *Kanisamys* cf. *potwarensis* (Parmar and Prasad, 2006; Parmar *et al.,* 2018). Therefore, the studied enamels are referred here to as the lower incisor of cf. *Kanisamys.*

VPL/AS/KU-2 cannot belong to the gerbilline, cricetine, sciurine, ctenodactyline or murine because all of these have two-layered uniserial enamel except for ctenodactyline which is characterised by multiserial/pauciserial enamel. The enamel of the fossil sample is very similar to that of rhizomyines in having a three-layered structure and thicker outer enamel with the presence of a ridge where longitudinal HSBs become transversely oriented. The cross-section of the incisor is triangular and the incisor is bigger. Kalthoff (2000) studied the incisor enamel microstructure of *Prokanisamys arifi* and found very similar features, except that it lacked the enamel ridge. As the fossil sample VPL/AS/KU-2 resembles the enamel microstructure of cf. *Kanisamys* (VPL/AS/R-2 and VPL/AS/R-6) from Ramnagar it is also referred here to as the genus cf. *Kanisamys.*

Rhizomys Gray, 1831

cf. *Rhizomys*

Locality and age: Moginand, Upper Siwalik (~ 4- 3.5 Ma- Early Pliocene).

Referred material: VPL/AS/M-20.

Internal structure of enamel- VPL/AS/M-20 four-layered uniserial enamel (Fig. 33). The outer and inner enamel are each divided into two layers. The outer enamel divided into OPE and IPE. OPE with radial enamel and IPE with tangential enamel. The inner enamel is divided into OPI and IPI. OPI with transversely arranged HSBs with angled IPM and IPI with longitudinally arranged HSBs with parallel IPM (Fig. 34A). Enamel 147µm thick and PE more than 25% of total enamel thickness (Table-3). In TS, prisms oval to flat (Fig. 34A). In LS, incisal bands inclined at 50° in PI and in the outer enamel prisms inclined at 70° (Fig. 34B). Band width 14µm.

Table-5. Linear and angular measurements of enamel microstructure of fossil incisors of Kanthro area (Late Pliocene).

SPECIMEN NUMBER	INCISOR CROSS-SECTION	TE (µm)	EI	II(°)	OI(°)	BW (µm)	α(°)	IPM INCLINATION	HSB ORIENTATION	PRISM CROSS SECTION IN PI	MODIFIED RADIAL ENAMEL	ENAMEL SURFACE
VPL/AS/K-1		98	0.19	45	80	2.5	90	Angled	Transverse HSB	Sub-round to oval	Absent	Smooth
VPL/AS/K-2	Oval	86	0.24	50	90	4.5	80	angled	Transverse HSB	Sub-round to oval	absent	Smooth
VPL/AS/K-3	Sub-triangular	64	0.21	20	45	5	60	Angled	Transverse (centre) and diagonal (lateral and mesial)	Oval to flattened	Absent	Grooved
VPL/AS/K-4	Oval	109	0.20	50	70	2.5	80	Angled	Transverse HSB	Sub-round to oval	Absent	Smooth
VPL/AS/K-5	Sub-triangular	141	0.22	15	95	4	70	Angled	Transverse HSB	Oval to flattened	Absent	Slightly wrinkled
VPL/AS/K-6		113	0.18	30	80	3.5	80	Angled	Transverse HSB	Oval to flattened	Absent	Smooth
VPL/AS/K-7		133	0.10	45	80	3	80	Angled	Diagonal HSB	Oval to flattened	Absent	Smooth
VPL/AS/K-8		142	0.19	40	80	3	70	Angled	Transverse HSB	Sub-round to oval	Absent	Smooth

Table-6. Evolutionary trend of incisor enamel microstructure observed in *Antemus-Progonomys-Mus* lineage.

Specimen	*Antemus* (13.2 -13.8 Ma)	*Progonomys* (11 -10 Ma)	*Mus* (4 -1.8 Ma)
HSB arrangement	Transverse	Transverse to slightly diagonal	Transverse (centre) to diagonal (lateral and mesial) to only diagonal
IPM inclination	Angled	Angled	Angled (close to perpendicular)
Prism cross-section	Round	Round to sub-round	Oval shaped
Prism packing	Loose	Loose	Tight

Comparison: The present incisor is not related to murids, cricetids, gerbillids and ctenodactylids because of its four-layered enamel structure. It shows affinity to *Rhizomys* because it is smooth and lacks a ridge on the enamel surface. It has a four-layered enamel microstructure with dominantly longitudinally aligned HSBs with parallel IPM in OPI and transversely aligned HSBs with angled IPM in IPI. Four-layered enamel microstructure with longitudinal HSBs is considered to be the most advanced enamel structure type (Kalthoff, 2000). Therefore, it is here assigned to cf. *Rhizomys*.

Family **Sciuridae** Fischer de Waldheim, 1817
Subfamily **Sciurinae** Hemprich, 1820
Tamias **Illiger**, 1811

Cf. *Tamias*

Locality and age: Tapar, Kachchh (11-10 Ma).

Referred material: VPL/AS/KU- 11, VPL/AS/KU-12, VPL/AS/KU-17.

External description of incisor enamel: The incisor is dark brown with a smooth enamel surface. Enamel and dentine are seen in the cross-section (Fig. 35A).

Internal structure of enamel: The enamel two-layered with uniserial HSBs in PI and radial enamel in PE (Fig. 36A). The total enamel thickness 107µm, PE is more than 20% (Table-2). In TS, prisms oval to flat (Fig. 36A) and decussate at 90° and IPM crystallites at an angle to the prisms in the third dimension (Fig. 36A). The transversely arranged HSBs are weakly inclined in the inner enamel and the outer enamel radial with parallel prisms and perpendicular IPM (Fig. 36A). In LS, incisal prism bands inclined at 10° in PI and outer enamel inclination 50°, band width 4µm (Fig. 36B).

Comparison: The enamel microstructures of the present specimens VPL/AS/KU-11, VPL/AS/KU-12 and VPL/AS/KU-17 are closely similar to sciurids in having less inclined bands, IPM running parallel to the prisms and IPM angled near EDJ or outer enamel surface where prisms bend (Boyde 1978; Wahlert and Koenigswald, 1985). As the sciurid fossils from Tapar, Kachchh are represented only by *Tamias* based on molar morphology (Bhandari *et al.,* 2021), the present incisors VPL/AS/KU-11, VPL/AS/KU-12 and VPL/AS/KU-17 are also assigned to cf. *Tamias.*

Family **Ctenodactylidae** Zittel, 1893
Sayimys **Wood**, 1937

Cf. *Sayimys*

Locality and age: Tapar, Kachchh (11-10 Ma, late Miocene).

Referred material: VPL/AS/KU-16.

External description of incisor enamel: VPL/AS/KU-16 light brown (Fig. 37B) with only enamel preserved.

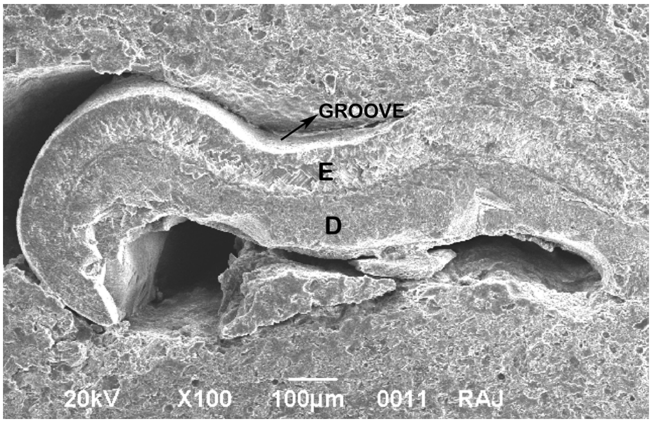

Fig. 26. SEM micrograph of fossil incisor VPL/AS/M-5 from Moginand area showing the sub- triangular cross-sectional view. E- Enamel, D- Dentine.

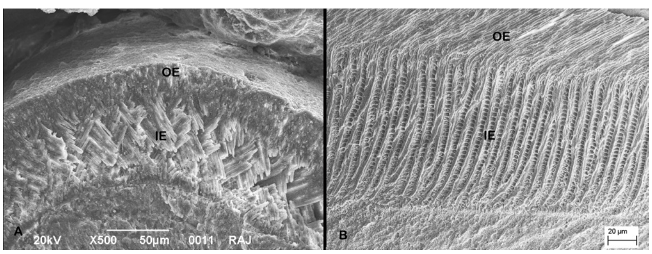

Fig. 27. SEM micrographs of fossil incisor VPL/AS/M-5 from Moginand area showing A. Transverse section, B. Longitudinal section.

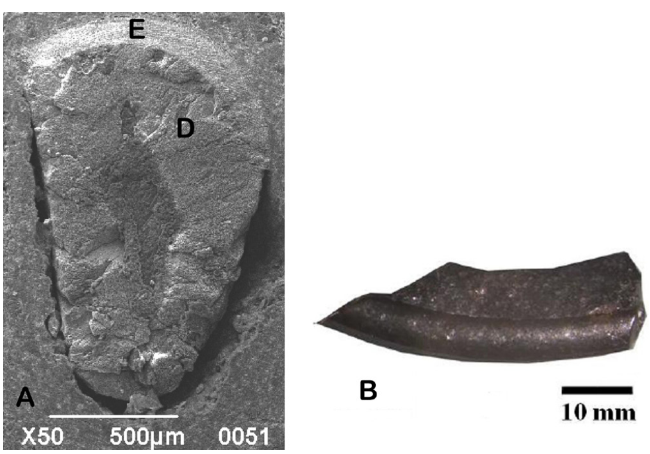

Fig. 28. A. SEM micrograph of fossil sample VPL/AS/R-3 from Ramnagar area showing oval-shaped cross-section, B. Microscopic image of incisor in side view with the tip of incisor well preserved.

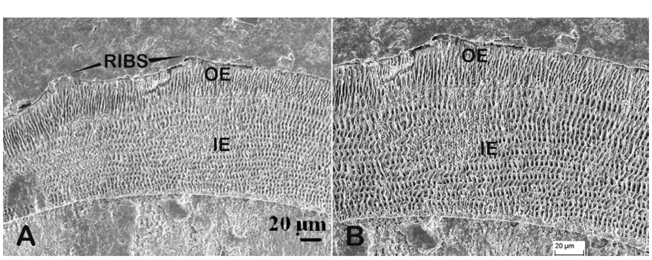

Fig. 29. SEM micrographs of fossil incisor (VPL/AS/R-4) from Ramnagar area showing A. Transverse section of enamel showing the presence of two ribs, B. Transverse section showing outer enamel and inner enamel.

Internal structure of enamel: VPL/AS/KU-16 two-three layers of prisms, displays the subtype-2 of multiserial HSBs, characterized by HSBs with sheet-like IPM and IPM crystallites forming acute angles with the direction of the prism crystallites (Fig. 38A). Anastomoses of IPM rare and transitional zones between two adjacent HSBs are well marked (Fig. 38B). Enamel is 191µm thick and PE comprises less than 20% of total enamel thickness (Table-2). In TS, prisms are oval in cross-section (Fig. 38B). In LS, incisal bands inclined at 40° in PI and 100° in outer enamel and band width 20µm (Fig. 39A & B).

Comparison: Ctenodactyloidea is the only group that shows a transition from pauciserial enamel to multiserial enamel. Ctenodactylids found from Oligocene onwards have multiserial enamel with acute-angled IPM (ex. *Leptotataromys*) and by the middle Miocene they acquired rectangular IPM in *Sayimys sivalensis* which also characterizes the extant species (Martin, 1992). As the sample VPL/AS/KU-16 has multiserial enamel microstructure with rectangular IPM, it is referred to here as cf. *Sayimys.*

DISCUSSION

Taxonomy based on enamel microstructure

Koenigswald and Clemens (1992) suggested a hierarchial scheme to understand the complexity of mammalian enamel and divided it into five levels of complexity according to the size of the structure involved: Crystallites, Prisms, Enamel types, Schmelzmuster and Dentition. The morphology and the patterns of organisation or packing of prisms and prism cross-sections are used to characterize various mammalian orders (Shobhusawa, 1952; Boyde, 1976; Kalthoff, 2000). Theoretically, dentitions and schmelzmusters can be used for the identification of mammals up to genus/species levels (Koenigswald and Clemens, 1992).

In the present work, various parameters of incisor enamel microstructure are used to differentiate taxa that have already been described by various authors (Wahlert, 1968; Boyde, 1978; Flynn, 1977, 1982; Patnaik, 2001, 2002, 2003a; Kalthoff, 2000, 2006; Koenigswald and Kalthoff, 2006). Incisor enamel microstructure features particularly useful in taxonomic identification are surface ornamentation, such as the presence of ribs (Cricetids), grooves (gerbillines) and ridges (rhizomyines) and incisor cross-section. Ctenodactylids show the transition from pauciserial to multiserial enamel type (Martin, 1995). Sciurids show uniserial enamel with three-layered microstructure having bands less inclined and IPM being parallel to the prisms and angled near EDJ or near the outer enamel surface where prisms bend (Boyde, 1978; Wahlert and Koenigswald, 1985). Flynn (*et al.,* 1985) reported species of *Democricetodon* with two enamel ribs and later Kalthoff (2000) also reported species of *Democricetodon* with more or less pronounced longitudinal enamel ribs. Rhizomyines are burrowing rodents which used their incisors for digging and prefer to live a subterranean life. Incisor enamel microstructure of rhizomyines is characterized by advanced form of enamel in lower incisors with three-four layered enamel structure. A ridge is formed at the centre due to the thickening of outer enamel in lower incisors in most spalacids (Flynn, 1982; Kalthoff, 2000; Patnaik, 2003a). Murines, which evolved from cricetids are one of the youngest, abundant and diverse groups (López-Antoñanzas *et al.,* 2019). Their incisors analysed in both lower and upper jaws show uniform and advanced features of enamel microstructure. The enamel surface is smooth with upper incisor having rounded to oval cross-section than lower incisor which shows oval cross-section. *Mus* lineage mostly comprises transversely arranged HSBs at the centre and diagonally arranged HSBs towards lateral and mesial sides with angled to perpendicular IPM and shows oval incisor cross-section. *Karnimata* lineage comprises mostly transversely arranged HSBs with angled IPM and triangular to sub-triangular incisor cross-section. Outer enamel is thin (less than 20%) in most of the murines except for the diggers like *Nesokia* and *Bandicota* which have thicker outer enamel i.e., (>30%). Upper and lower incisors can also be differentiated based on incisor enamel microstructure. The studied features of enamel microstructure of murine rodents are in accordance with the features noticed by earlier workers (Koenigswald, 1985; Martin, 1992, 1993, 1994; Kalthoff, 2000; Patnaik, 2002).

Incisors of extant mice (*Mus musculus*) and rats (*Rattus, Golunda, Millardia, Bandicota*, *Nesokia*, etc.) were analysed to create a reference data set for comparing the fossil specimens. It was observed that *Antemus- Progonomys- Mus* lineage represents oval cross-section and *Karnimata* lineage (including *Golunda, Millardia, Bandicota*, *Nesokia, Rattus*) represents triangular cross-section. In respect to their body size, *Antemus, Progonomys* and *Mus* have smaller incisors, while *Millardia* and *Cremnomys* have medium-sized incisors. Large robust incisors characterise forms such as *Rattus, Bandicota* and *Nesokia.*

Incisor enamel microstructural measurements of extant species related to genus *Mus* show variations in enamel thickness from 92 to 112 µm in lower incisors and 62 to 88 µm in upper incisors. Incisal band inclination of lower incisors is more (35° to 45°) than that in upper incisors (20° to 25°). Decussation angle increases from enamel-dentine junction to outer enamel surface and shows variation from 70° to 90°. *Antemus- Progonomys- Mus* lineage related species show mostly transverse to diagonally oriented HSBs with angled to perpendicular IPM, while *Karnimata* lineage (including *Golunda, Millardia, Bandicota*, *Nesokia, Rattus)* shows mostly transversely oriented HSBs with angled IPM. Incisor enamel microstructural measurements of species related to *Rattus* including *Rattus rattus, Golunda ellioti, Millardia meltada* show variation in enamel thickness from 116 to 139 µm in upper incisors and 64 to 150 µm in lower incisors. Incisal band inclination of lower incisors is more (15° to 40°) than that in upper incisors (15° to 30°) and decussation angle varies from 60° to 70° in upper incisors and from 70° to 90° in lower incisors. *Nesokia* and *Bandicota* have thicker outer enamel that varies from 36% to 44%. The enamel thickness varies from 149 to 152 µm, incisal band inclination varies from 30° to 35° and decussation angle varies from 80° to 90°. Although the linear and angular measurements of enamel microstructure are overlapping, it can still be differentiated broadly at least up to the genus level.

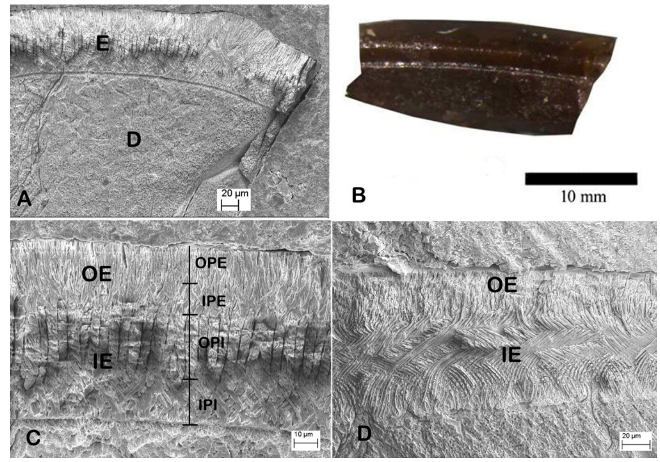

Fig. 30. SEM micrographs (A, C & D) and a microscopic image (B) of fossil incisor (VPL/AS/R-6) from Ramnagar area showing, A. Transverse section of incisor enamel and dentine with ridge present on the enamel surface (Scale-20µm), B. Side view of fossil incisor, C. Transverse section of incisor showing four-layered enamel structure (Scale-10µm), D. Longitudinal section of incisor showing decussating prisms (Scale-20µm). OE- Outer enamel: OPE- Outer Portio Externa, IPE- Inner Portio Externa; IE- Inner enamel: OPI- Outer Portio Interna, IPI- Inner Portio Interna.

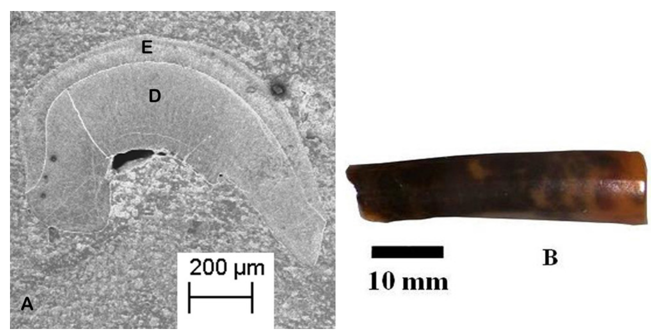

Fig. 31. A. SEM micrograph of fossil incisor VPL/AS/KU-2 from Kachchh area showingcross-sectional view, B. Microscopic image of incisor in top view showing smooth enamel surface.

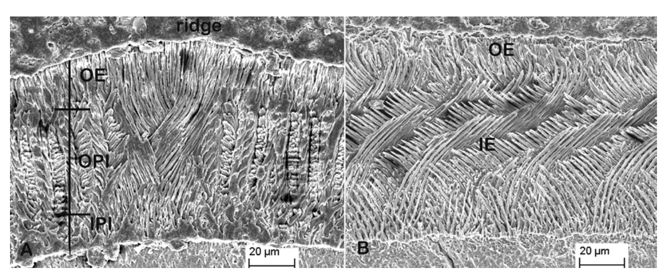

Fig. 32. SEM micrographs of fossil incisor VPL/AS/KU-2 from Kachchh area showing, A. Transverse section showing three-layered enamel structure with a ridge present in the centre of the enamel surface, B. Longitudinal section showing decussating prisms.

From the middle Miocene of Ramnagar area, many rodent taxa such as Murinae (*Antemus*), Gerbillinae (*Myocricetodon*), Cricetinae (*Megacricetodon, Punjabemys*), Rhizomyinae (*Kanisamys*), Scuirinae (*Tamias*), Ctenodactylidae (*Sayimys*) have been described based on molar morphology (Parmar and Prasad, 2006; Sehgal and Patnaik, 2012; Parmar *et al.,* 2015, 2017, 2018). Three sub-families namely, Murinae (cf.

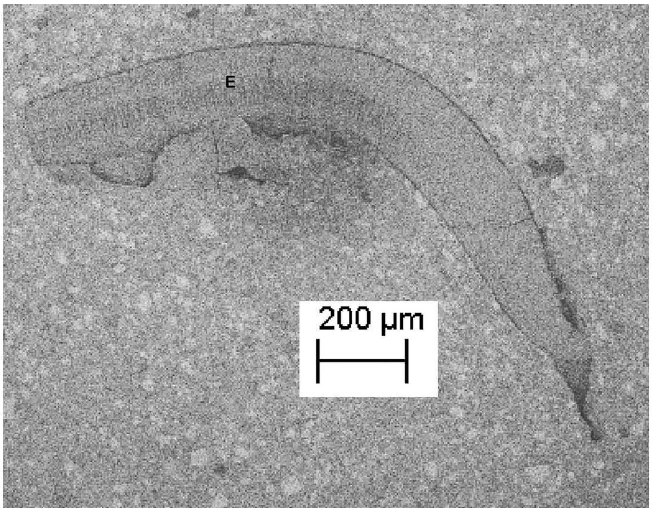

Fig. 33. SEM micrograph of fossil incisor VPL/AS/M-20 from Moginand area showing enamel (E) structure only.

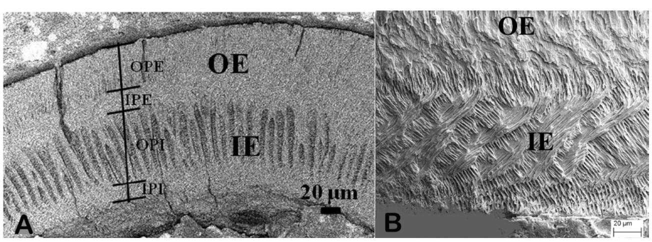

Fig. 34. SEM micrographs of fossil incisor VPL/AS/M-20 from Moginand area showing A. Transverse section showing four-layered enamel structure, B. Longitudinal section. OE- Outer enamel, OPE- Outer Portio Externa, IPE- Inner Portio Externa, OPI- Outer Portio Interna, IPI- Inner Portio Interna.

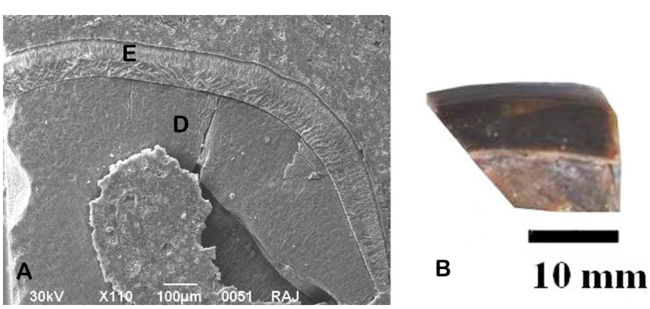

Fig. 35. A. SEM micrograph of fossil incisor VPL/AS/KU-17 from Kachchh area showing enamel and dentine in cross-section, B. Microscopic image of fossil incisor in side view showing smooth enamel surface. E- Enamel, D- Dentine.

Antemus), Cricetinae (cf. *Democricetodon*) and Rhizomyinae (cf. *Kanisamys*) are identified here from Ramnagar on the basis of their incisor enamel microstructure.

From the late Miocene deposits of Kachchh, *Progonomys morganae* (murid), *Tamias urialis* (sciurid), *Prokanisamys, Kanisamys* (Rhizomyinae), *Sayimys sivalensis* (ctenodactylid), *Democricetodon* (cricetid), *Dakkamys* (gerbillid) were reported based on molar morphology (Bhandari *et al.,* 2021). Of these two sub-families, namely Murinae (cf. *Progonomys*) anf Rhizomyinae (cf. *Kanisamys*) and two families, namely Ctenodactylidae (cf. *Sayimys*) and Sciuridae (cf. *Tamias*) are here identified based on their incisor enamel microstructure, Kachchh

In the Pliocene, murines were abundant and widespread. Murines are divided into two clades- *Mus* lineage and *Karnimata* lineage (Jacobs, 1978). From the early Pliocene deposits of Moginand area *Mus, Golunda tatroticus, Cremnomys, Millardia, Dilatomys moginandensis,* and *Abudhabia* were reported based on molar morphology (Patnaik, 1997, 2001, 2002, 2003b). In this work, based on incisor enamel microstructural studies three sub-families namely Murinae (cf. *Nesokia/Bandicota,* cf. *Millardia,* cf. *Mus,* cf. *Golunda*), Gerbillinae (cf. *Abudhabia*) and Rhizomyinae (cf. *Rhizomys*) have been identified at Moginand.

From the late Pliocene deposits of Devni Khadri area *Golunda kelleri, Mus flynni, Mus jacobsi,* and *Abudhabia* and from Kanthro area *Parapelomys robertsi, Mus flynni, Golunda kelleri, Golunda, Millardia, Cremnomys, Bandicota sivalensis,* and *Abudhabia* were reported based on molar morphology (Patnaik, 1997, 2001, 2002, 2003b; Patnaik *et al.,* 2018). *Golunda* from Kanthro shows central and deep grooves on the enamel surface of its upper incisor. Fossil samples from the late Pliocene are assigned here under *Mus* and *Karnimata* lineages which include cf. *Nesokia/ Bandicota,* cf. *Mus* and cf. *Golunda.*

Evolutionary trends and phylogenetic relationship

Spatial arrangement of HSBs: Phylogeny involves the evolution of species or groups of species. In this research work, evolution has been observed in the incisor enamel microstructure of *Mus* and *Karnimata* lineages and rhizomyine. Except for cf. *Sayimys* from Kachchh**,** all other examined rodent taxa, both fossil and extant, show uniserial enamel in which HSBs of the inner enamel are aligned in three directions- transverse, diagonal and longitudinal. Transverse HSBs represent the most generalised form and longitudinal alignment is the most evolved state (Kalthoff, 2000). Rodents studied in this research work show homogenous enamel microstructure, i.e., all have uniserial enamel with dominant transversely aligned HSBs and less dominant diagonally aligned HSBs. Murines is the only group that is present from middle Miocene to recent and in which evolution has been observed in the alignment of HSBs from transverse to partly transverse and partly diagonal to completely diagonal. Samples studied from the middle Miocene (cf. *Antemus*) show the dominantly transverse alignment of HSBs which is in contrast to the recent mice species (*Mus musculus*) having partly diagonal and partly transverse HSBs to completely diagonal HSBs in rats (*Rattus*). The highly derived longitudinal HSBs have been found only in rhizomyines among all the studied fossil and extant taxa. Further, evolution in the inner enamel has been observed where it is divided into IPI (inner portio interna) and OPI- outer portio interna. This type of enamel is the most advanced state and is found only in rhizomyines. Stratigraphically younger taxa show advanced state of alignment of HSBs. It has been observed that the lower incisor HSBs are mostly inclined to a greater degree than upper incisors indicating that these were biomechanically more evolved. Further, rodents examined in this research show increase in decussation angle from middle Miocene (low angle ~50°) to recent (high angle ~ 90°).

Inclination of the IPM to prisms: IPM either runs parallel to prisms or at some angle or perpendicular to the prisms. Former condition is a primitive state and the latter is the most derived state. On the basis of inclination of the IPM, the inner enamel layer is divided into IPI (angled IPM to the prisms) and OPI (prism parallel IPM). Biomechanically, the inclination of the IPM to prisms is significant. Perpendicular inclination of IPM in the third dimension gives two-dimensional construction of enamel a strong consolidation against spreading of microcracks (Pfretzschner, 1988). In all the studied samples both fossil and extant, evolution in the inclination of IPM angle from low to high has been observed. Recent species of *Mus* shows almost perpendicular IPM and rhizomyines show two-layered inner enamel which is the most advanced form (Kalthoff, 2000).

Prism cross-section: Another important enamel feature is prism cross-section. Prisms are rounded, sub-rounded, oval, lancet or flattened in shape. Round prism cross-section is the original form and oval to lancet-shaped prisms are the advanced forms (Kalthoff, 2000). This evolutionary trend of prism cross-section from round to oval has also been observed in the studied samples in both fossil (cf. *Antemus*) and recent forms (*Mus musculus*) (Table-6).

From the Pliocene sediments, two upper incisor specimens were identified as cf. *G. tatroticus* (early Pliocene-Moginand) and cf. *G. kelleri* (late Pliocene- Devni Khadri) and were compared with incisors of extant *G. elliotí.* Incisor enamel microstructure of all the three samples is almost similar but the variation lies in the position of groove. In cf. *G. tatroticus* (Moginand) groove is lateral, whereas groove of cf. *G. kelleri* is comparatively deep and present in the centre (Fig.40). Patnaik (2001) observed that upper incisors of *G. kelleri* from Kanthro closely resemble *G. ellioti* in having laterally grooved enamel. Since cf. *G. tatroticus* also has laterally grooved enamel (Fig.26) the probable lineage would be cf. *G. tatroticus- G. kelleri* (Kanthro) - *G. ellioti*, while cf. *G. kelleri* (Devni Khadri) could belong to a different offshoot.

Feeding and habitat preferences

Incisor enamel of rodents is the hardest tissue which is formed in a way that allows the animal in cutting hard materials like copper/aluminium wires, dig holes, feed on hard nuts/seeds etc. The chisel-shaped sharp incisor structure is composed of outer radial enamel and inner decussating enamel. Outer radial enamel acts as a cutting edge and inner enamel acts as a strengthening device, while the IPM in the third direction helps in the prevention of crack propagation (Koenigswald and Pfretzschner, 1987). The presence of modified radial enamel near the enamel-dentine junction is an adaptation to prevent structural failure under extreme stress conditions during burrowing activity, underground feeding or feeding on abrasive materials or eating fibre-rich plants, etc. (Kalthoff and Mors, 2021). It is assumed that like extant wild variety of mice (*Mus*) its ancestor cf. *Antemus*

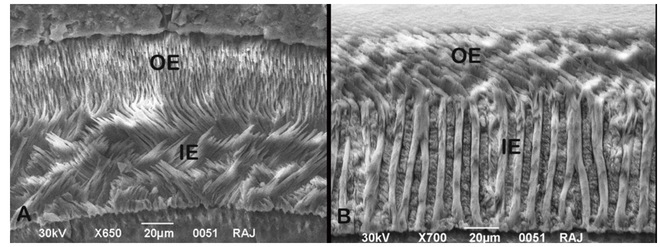

Fig. 36. SEM micrographs of fossil incisor VPL/AS/KU-17 from Kachchh area showing A. Transverse section, B. Longitudinal section.

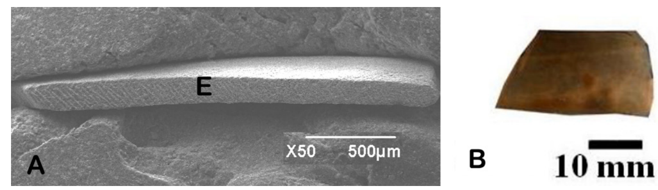

Fig. 37. A. SEM micrograph of fossil incisor VPL/AS/KU-16 from Kachchh area showing enamel in cross-section, B. Microscopic image of the top view of the incisor showing smooth enamel surface. E- Enamel.

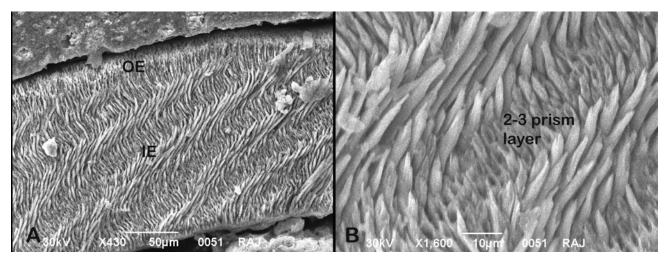

Fig. 38. A & B. SEM micrographs of transverse section of fossil incisor VPL/AS/KU-16 from Kachchh showing subtype-2 multiserial enamel. The two-layered enamel structure with outer radial enamel and decussating inner enamel with 2-3 prism wide HSBs.

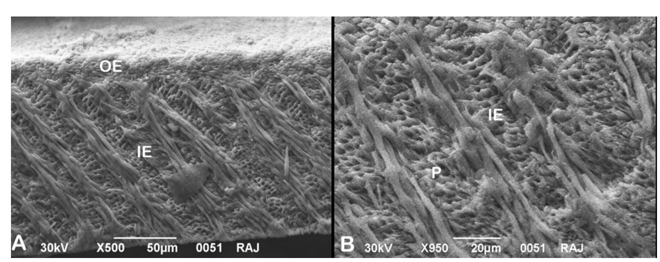

Fig. 39. A & B SEM micrographs of longitudinal sections of fossil incisor VPL/AS/KU-16 from Kachchh area showing subtype-2 multiserial enamel.

Fig. 40. From left to right- fossil upper incisor samples VPL/AS/M-2, VPL/AS/K-3 and extant species VPL/AS/GE1, *Golunda ellioti* showing position of groove on enamel surface. (Scale- 200µm)

Fig. 41. A. Upper incisor sample VPL/AS/M-2 from Early Pliocene deposits of Moginand showing laterally grooved structure, B. Upper incisor sample VPL/AS/K-3 from Late Pliocene deposits of Kanthro showing central position of groove.

from middle Miocene deposits of Ramnagar also fed on seeds, grains small invertebrates and insects as both show very similar enamel microstructure (thin outer enamel and high inclination of HSBs). Middle Miocene floral and faunal assemblages around Ramnagar represent a warm and humid tropical environment with frequent swampy conditions and an abundance of the forested environment near the banks of a fluvial system, combined with the occurrence of a more open woodland/bushland environment (Singh *et al.,* 2018). Middle Miocene muroid rodent *Antemus* preferred an insect-dominated carnivorous diet and most likely lived in forest habitats (Tiphaine *et al.*, 2013 Flynn, 2003). Stable isotope values and microwear studies suggest a fruit/insect diet for *Antemus chinjiensis* (Kimura, *et al.,* 2013; Patnaik, 2015) whereas cricetids show a wide range of diet preferences from herbivory, omnivory to insectivory (Singh *et al.,* 2018). Though rhizomyines do not show modified radial enamel, their thicker outer enamel depicts burrowing nature (Kalthoff, 2000; Patnaik, 2003a). Spalacids (rhizomyines) of the middle Miocene primarily thrived onC_3 diet (browsers) but might also have consumed seeds, roots and leaves and lived in sub-tropical forest conditions (Patnaik, 2015 Singh *et al.,* 2018). Therefore, their dietary habits are relatable to their habitats implying that all three identified sub-families namely, murine, cricetine and rhizomyine from middle Miocene deposits of Ramnagar area lived together in a warm and humid forest environment.

In the late Miocene, *Antemus* separated into two clades: one was *Progonomys* clade and the other was *Karnimata* clade. *Karnimata* clade is better adapted to C_4 grasslands than *Progonomys* clade because of their bigger body mass (Kimura *et al.,* 2013). *Progonomys* prefers a plant-dominated omnivorous diet (Tiphaine *et al.,* 2013). In the late Miocene period, the global climate entered into cooler and drier conditions with the dominance of C_4 grasslands in the Indian sub-continent (Patnaik and Prasad, 2016) and during this time the cricetids were replaced by murids possibly due to monsoon intensification and dietary shift (Patnaik, 2003b). Cricetids are mixed feeders and spalacids are grazers feeding mainly on seeds, nuts and leaves (Patnaik, 2015). It appears that fossils identified as cf. *Progonomys are* used to feed on a softer plant dominated diet because there is no stress related features like modified radial enamel or thick outer enamel in their enamel microstructure. Spalacids fed on hard substances and were diggers too as evidenced by the existence of thick outer enamel and longitudinal HSBs.

Pliocene murid rodents lived mainly in broad ecological habitats. Today, *Nesokia* and *Bandicota* prefer irrigated croplands with moist sub-soil throughout the year and they prefer to eat vegetation, grains and earthworms (Patnaik, 2003b). *Millardia* also prefers cultivated fields/woody grasslands, sometimes heavy scrubs/rocks and are mixed feeders of C_3 diet (seeds, grass, insects), and *Mus* is also a mixed feeder (C_3 diet) (Patnaik, 2003b). *Abudhabia* could have lived in arid conditions, and *Golunda* is a grazer and fed on insects/seeds and prefers to live in sandy bushlands (Patnaik, 2003b). *Rhizomys* is adapted to subterranean life and prefers to live in burrows dug mostly on the sides of stream banks/open grass-covered ground (Prater, 1971; Patnaik, 1995; 2015; Patnaik and Sahni, 2000). Fossil samples from the Pliocene period belong mostly to *Mus* or *Karnimata* lineage and these were mainly mixed feeders and their enamel microstructural features like thin outer enamel, a thick layer of HSBs, modified radial enamel (found only in a few samples) reveal that they likely fed on a variety of plant-dominated diet. *Nesokia* and *Bandicota* have thick outer enamel and like the present-day species, their ancestors also might have used their incisors to dig burrows. Therefore, the dietary habits of different rodent species studied here are reflected in their incisor enamel microstructure suggesting the presence of different ecological niches ranging from wooded grasslands to sandy bushlands during Pliocene.

CONCLUSIONS

1. Based on the incisor enamel microstructural studies, the middle Miocene Ramnagar rodents can be assigned to three muroid sub-families, namely, Murinae (cf. *Antemus*), Cricetinae (cf. *Democricetodon*) and Rhizomyinae (cf. *Kanisamys*). The late Miocene Kachchh rodents belong to two muroid sub-families, namely, Murinae (cf. *Progonomys*), Rhizomyinae (cf. *Kanisamys*), and to two families, i.e., Ctenodactylidae (cf. *Sayimys sivalensis*) and Sciuridae (cf. *Tamias*). The early Pliocene Moginand and late Pliocene Kanthro and Devni Khadri sites have yielded taxa belonging to Murinae (cf. *Nesokia,* cf. *Millardia,* cf. *Mus,* cf. *Bandicota,* cf. *Golunda*), Gerbillinae (cf. *Abudhabia*) and Rhizomyinae (cf. *Rhizomys*).
2. Cricetids show uniserial enamel with partly diagonal and partly transverse HSBs, angled to parallel IPM and thin outer enamel. Cricetids are differentiated from other rodent groups based on surface ornamentation on incisors.
3. Murines show uniserial enamel with mostly transversely to partly transverse and partly diagonally arranged HSBs with angled to perpendicular IPM. Overall outer enamel is thin except for some diggers like *Nesokia* and *Bandicota* which show thicker outer enamel.
4. Spalacids show the most advanced type of uniserial enamel with three- to the four-layered enamel structure. A ridge is usually present on the enamel surface. Outer enamel is thickly occupying almost 35-40% of total enamel thickness and is divided into two parts. Inner enamel is also divided into two parts one with transverse HSBs and angled IPM and the other with longitudinal HSBs and parallel IPM.
5. Gerbillines show uniserial enamel microstructure with

transverse to diagonally arranged HSBs and angled IPM. Groove/sulcus is present on the enamel surface of upper incisors and a small notch like structure is present on the mesial side of the enamel.

6. In *Antemus-Progonomys-Mus* lineage, *Antemus* shows primitive enamel features such as rounded prism cross-section, transverse HSBs, angled IPM than in *Progonomys* while *Mus* shows most advanced enamel features such as oval prism cross-section, transverse and diagonal HSBs, and almost perpendicular IPM.
7. Based on the position of the groove on the enamel surface, a possible new lineage comprises cf. *G. tatroticus*- *G. kelleri* (Kanthro) - *G. ellioti*.
8. Biomechanically, cf. *Antemus* identified from the Middle Miocene and a few other murine rodents from Pliocene onwards show modified radial enamel indicating their dietary habits related to hard substances.
9. Spalacids identified here show thicker outer enamel indicating burrowing behaviour. Some murines like *Nesokia* and *Bandicota* also show thick outer enamel suggesting digging and burrowing behaviour.

ACKNOWLEDGEMENTS

Ankita Singla was supported by CSIR and DST-DAAD, Rajeev Patnaik was supported by MoES/P.O. (Geosci)/46/2015, DST-DAAD and SERB-HRR/2018/000063 for fieldwork in the Siwaliks and Kachchh. We would like to extend our thanks to Prof. Matthias Epple, Dr Oleg Prymak, Dr Nataniel Bialas and Dr Kateryna Loza for their help with SEM analyses of some specimens.

REFERENCES

Barry, J. C. and Flynn, L. J. 1990. Key biostratigraphic events in the Siwalik sequence. In European Neogene mammal chronology, 557-571.

Bhandari, A., Bajpai, S., Flynn, L. J., Tiwari, B. N. and Mandal, N. 2021. First Miocene rodents from Kachchh, western India. Historical Biology, 1-9.

Boyde, A. 1976. Enamel structure and cavity margins. Operative Dentistry, 1(1): 13-28.

Boyde, A. 1978. Development of the structure of the enamel of the incisor teeth in the three classical subordinal groups of the Rodentia. Development, function and evolution of teeth, 43-58.

Escala, M. C. and Gállego, L. 1977. Systematic usefulness of lower incisor enamel in Muridae (Rodentia). Journal of Mammalogy, 58(1): 25-31.

Flynn, L. J. 1977. Enamel microstructures of cricetid and heteromyid rodent incisors and their importance in rodent phylogeny. M.Sc. Thesis. University of Arizona.

Flynn, L. J. 1982. Biostratigraphy and systematics of Siwalik Rhizomyidae (Rodentia). Ph.D. Thesis.University of Arizona.

Flynn, L. J. 2003. Small mammal indicators of forest paleoenvironment in the Siwalik deposits of the Potwar Plateau, Pakistan. Deinsea, 10(1): 183-196.

Flynn, L. J., Jacobs, L. L. and Lindsay, E. H. 1985. Problems in muroid phylogeny: relationship to other rodents and origin of major groups. In: Evolutionary relationships among rodents, 589-616.

Jacobs, L. L. 1978. Fossil rodents (Rhizomyidae & Muridae) from Neogene Siwalik deposits, Pakistan. Museum of North Arizona, Bulletin, 52: 1-103.

Kalthoff, D. C. and Mörs, T. 2021. Biomechanical adaptations for burrowing in the incisor enamel microstructure of Geomyidae and Heteromyidae (Rodentia: Geomyoidea). Ecology and Evolution.11(14): 9447–9459.

Kalthoff, D. C. 2000. The enamel microstructure in the incisors of hamster-like rodents and other myomorpha (Rodentia, Mammalia). Palaeontographica Section A, 1-193.

Kalthoff, D. C. 2006. Incisor enamel microstructure and its implications to higher-level systematics of Eurasian Oligocene and Early Miocene hamsters (Rodentia). Palaeontographica Section A, 67-80.

Kimura, Y., Jacobs, L. L., Cerling, T. E., Uno, K. T., Ferguson, K. M., Flynn, L. J. and Patnaik, R. 2013. Fossil mice and rats show isotopic evidence of niche partitioning and change in dental ecomorphology related to dietary shift in Late Miocene of Pakistan. PLoS One, 8(8): e69308.

Koenigswald, W. V. and Clemens, W. A. 1992. Levels of complexity in the microstructure of mammalian enamel and their application in studies of systematics. Scanning Microscopy, 6(1): 16.

Koenigswald, W. V. and Kalthoff, D. C. 2006. The enamel microstructure of molars and incisors of Paleogene and early Neogene rodents from Mongolia. Annalen des Naturhistorischen Museums in Wien. Serie A für Mineralogie und Petrographie, Geologie und Paläontologie, Anthropologie und Prähistorie, 291-312.

Koenigswald, W. V. and Pfretzschner, H. U. 1987. Hunter-Schreger-Bänder in Zahnschrnelz von Säugetieren: Anordnung und Prismenverlauf. (Hunter-Schreger bands in the mammalian tooth enamel: orientation and direction of prisms). Zoomorphology , 106 (6): 329-338.

Koenigswald, W. V. and Pfretzschner, H. U. 1991. Biomechanics in the enamel of mammalian teeth. In:Schmidt-Kittler N, Vogel K (eds). Constructional Morphology and Biornechanics, Springer-Verlaq, Berlin and Heidelberg.pp.113-125.

Koenigswald, W. V. 1980. Schmelzstruktur und Morphologie in den Molaren der-Arvicolidae (Rodentia). Abhandlungen Senckenbegische Naturforschende Gesellschaft, 539: 1-129.

Koenigswald, W. V. 1985. Evolutionary trends in the enamel of rodent incisors. In: W. P. Luckett, and J. L. Harten- berger, Eds., Evolutionary Relationships among Rodents, a Multidisciplinary Analysis, A Life Sciences, NATO ASI Series, 1985, pp. 403-422..

Korvenkontio, V. A. 1934. Microscopic examinations of rodent incisives with reference to the enamel structure of the molar teeth. In Annales zoologici societatis zoologicae-botanicae fennicae Vanamo, 2: p-1.

Kumar, K., Loyal, R. S. and Srivastava, R. 1997. Eocene rodents from new localities in Himachal Pradesh, Northwest Himalaya, India: biochronologic implications. Journal Geological Society of India, 50: 461-474.

Lehner, J. and Plenck, H. 1936. Die Zahne. In: Handbuch der mikroskopischen Anatomic des Menschen 5/3, W. v. Mrtlendorff, ed. 447-708, Berlin.

López-Antoñanzas, R., Flynn, L. J. and Knoll, F. 2013. A comprehensive phylogeny of extinct and extant Rhizomyinae (Rodentia): evidence for multiple intercontinental dispersals. Cladistics, 29(3): 247-273.

López-Antoñanzas, R., Renaud, S., Peláez-Campomanes, P., Azar, D., Kachacha, G. and Knoll, F. 2019. First levantine fossil murines shed new light on the earliest intercontinental dispersal of mice. Scientific Reports, 9(1): 1-16.

Martin, T. 1992. Schmelzstruktur in den Inzisiven alt-und neuweltlicher hystricognather Nagetiere. Palaeovertebrata, Mémoire extraordinaire, 1-168.

Martin, T. 1993. Early rodent incisor enamel evolution: phylogenetic implications. Journal of Mammalian Evolution, 1(4): 227-254.

Martin, T. 1994. African origin of caviomorph rodents is indicated by incisor enamel microstructure. Paleobiology, 20(1): 5-13.

Martin, T. 1995. Incisor enamel microstructure and phylogenetic interrelationships of Pedetidae and Ctenodactyloidea (Rodentia). Berliner Geowissenschaftliche Abhandlungen, 16: 693-707.

Parmar, V. and Prasad, G. V. R. 2006. Middle Miocene rhizomyid rodent (Mammalia) from the Lower Siwalik Subgroub of Ramnagar, Udhampur District, Jammu and Kashmir, India. Neues Jahrbuch für Geologie und Paläontologie-Monatshefte, 371-384.

Parmar, V., Prasad, G. V. R., Kumar, J., Malik, M. A. and Norboo, R. 2015. Cricetid rodents from the Lower Siwalik Subgroup of Jammu, India: biochronological significance. Palaeoworld, 24(3): 324-335.

Parmar, V., Magotra, R., Norboo, R. and Prasad, G. V. R. 2017. Rodent-based age appraisal of the Lower Siwalik Subgroup of Kalaunta, Ramnagar, Jammu, India. Alcheringa: An Australasian Journal of Palaeontology, 41(1): 124-133.

Parmar, V., Prasad, G. V. R. and Norboo, R. 2018. Middle Miocene small mammals from the Siwalik Group of Northwestern India. Journal of Asian Earth Sciences, 162: 84-92.

Patnaik, R. 1995. Micromammal-based palaeoenvironment of Upper Siwaliks exposed near Village Saketi, HP. Journal of Geological Society of India (Online archive from Vol 1 to Vol 78), 46(4): 429-437.

Patnaik, R. 1997. New murids and gerbillids (Rodentia, Mammalia) from Pliocene Siwalik sediments of India. Palaeovertebrata, 26(1-4): 129-165.

Patnaik, R. 2001. Late Pliocene Micromammals from Tatrot Formation (Upper Siwaliks) exposed near village Saketi, Himachal Pradesh, India. Palaeontographica Abteilung A, 261(1-3): 55-81.

Patnaik, R. 2002. Enamel ultrastructure of some fossil and extant murid rodents from India: functional, phylogenetic and taxonomic implications. Paleontological Research, 6(3): 239-258.

Patnaik, R. 2003a. Tooth Enamel Microstructure in some fossil Gerbillids and Rhizomyids from India: Functional and Taxonomic significance, Archives of comparative Biology of Tooth Enamel, 8: 59-66.

Patnaik, R. 2003b. Reconstruction of Upper Siwalik palaeoecology and palaeoclimatology using microfossil palaeocommunities. Palaeogeography, Palaeoclimatology, Palaeoecology, 197(1-2): 133-150.

Patnaik, R. 2015. Diet and habitat changes among Siwalik herbivorous mammals in response to Neogene and Quaternary climate changes: An appraisal in the light of new data. Quaternary International, 371: 232-243.

Patnaik, R. and Prasad, V. 2016. Neogene climate, terrestrial mammals and flora of the Indian Subcontinent. In Proc. Indian Natural Science Academy, 82: 605-615.

Patnaik, R. and Sehgal, R. 2012. New muroid rodent and Sivapithecus dental remains from the Lower Siwalik deposits of Ramnagar (J&K, India): Age implication. Quaternary International, 269: 69-73.

Patnaik, R. and Sahni, A. 2000. Palaeobiogeography of Pliocene Siwalik murid and Gerbillid rodents. Geological Survey of India Miscellaneous Publications, 64: 43-47.

Patnaik, R., Kotla, S. S., Singh, N. P., Singla, A. and Kaur, J. 2018. A new murid rodent assemblage from the Upper Siwaliks, Himachal Pradesh, India: biostratigraphic, phylogenetic and palaeobiogeographic implications. Journal of Asian Earth Sciences, 162: 93-106.

Pfretzschner, H. U. 1988. Structural reinforcement and crack propagation in enamel. In Teeth Revisited. Proceedings of the VIIth International Symposium on Dental Morphology, Museum d'Histoire Naturelle, Paris, 53: 133-143.

Pfretzschner, H. U. 1994. Biomechanik der Schmelzmikrostruktur in den Backenzähnen von Großsäugern. Palaeontographica Abteilung A, 234: 1-88.

Prater, S. H. 1971. The Book of Indian Animals, 3rd edition. Bombay Natural History Society, Oxford University Press, Bombay, p-324.

Sahni, A. 1980. SEM studies of Eocene and Siwalik rodent enamels. Geoscience Journal, 1/2: 21-30.

Schroeder, H. E. 1987. Orale strukturbiologie, Entwicklungsgeschichte, Struktur und funktion normaler Hart-und Weichgewebe der Mundhohle und des Kiefergelenks. Thieme Verlag, Stuttgart, New York.

Shobusawa, M. 1952. Vergleichende Untersuchungen über die Form der Schmelzprismen der Säugetiere. Comparisons of the shape of mammalian enamel prisns. Okajimas Folia Anatomica Japonica, 24(5-6): 371-392.

Singh, N. P., Gilbert, C. C., Patel, B. A. and Patnaik, R. 2018. The taphonomy and palaeoecology of the Middle Miocene hominoid locality of Ramnagar (Jammu and Kashmir, India). Journal of Asian Earth Sciences, 162: 69-83.

Tiphaine, C., Yaowalak, C., Cyril, C., Helder, G. R., Jacques, M., Paul, T., Monique, V.L., Laurent, V. and Vincent, L. 2013. Correlated changes in occlusal pattern and diet in stem Murinae during the onset of the radiation of Old World rats and mice. Evolution, 67(11): 3323-3338.

Tomes, J. 1850. On the structure of the dental tissues of the order rodentia. Philosophical Transactions of the Royal Society of London, 140: 529-567.

Wahlert, J. H. 1968. Variability of rodent incisor enamel as viewed in thin section, and the microstructure of the enamel in fossil and recent rodent groups. Breviora, 309: 1-18.

Wahlert, J. H. and Koenigswald, W. V. 1985. Specialized enamel in incisors of eomyid rodents. American Museum Novitiates, 2832.